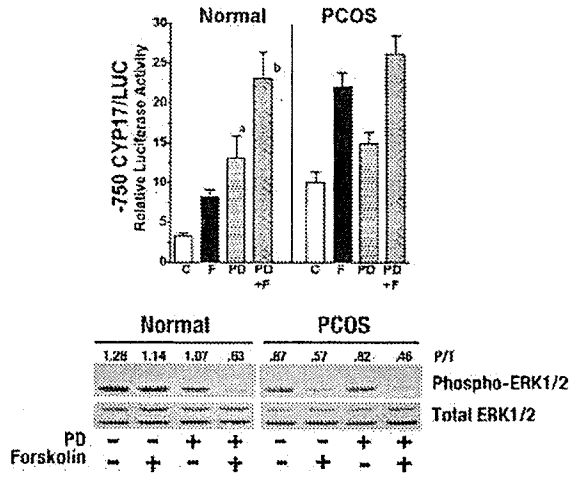

Fig. 6. Inhibition of the ERK1/2 MAPK Pathway with the MEK1 Inhibitor PD Differentially Regulates *CYP17* Promoter Activity in Normal and PCOS Theca Cells

Upper panel: Fourth-passage theca cells isolated from normal or PCOS patients were transiently transfected with a pGL3 LUC construct containing −750 to +44 bp of the *CYP17* promoter. After transfection, the cells were treated with vehicle (C) or 7.5 μM forskolin (F) with and without the 25 μM PD. Seventy-two hours thereafter, the cells were harvested and LUC activity assayed. Data are presented as relative LUC activity that has been corrected for β-Gal activity. Data represent the mean ± SEM of experiments performed with triplicate cultures of theca cells isolated from five independent normal and PCOS patients. In normal theca cells, inhibition of ERK1/2 signaling using PD augmented both basal (a, $P < 0.05$) and forskolin (b, $P < 0.05$) stimulated −750 CYP17/LUC promoter activity. In contrast, −750 CYP17/LUC promoter activity was not significantly increased in response to PD treatment in PCOS theca cells. *Bottom panel:* To compare the effects of PD on ERK1/2 phosphorylation in normal and PCOS theca cells, fourth-passage theca cells propagated from normal and PCOS patients were grown to confluent and transferred into serum-free medium with vehicle (C) or 7.5 μM forskolin (F) in the presence or absence of 25 μM PD. Twenty-four hours thereafter, the cells were harvested, and immunoblot analysis was performed using 35 μg of whole cell extract and antibodies specific for phosphorylated ERK1/2 (Phospho-ERK 1/2) and total ERK1/2.

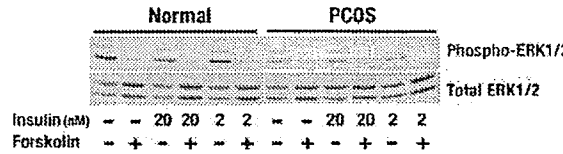

Fig. 7. The Activation State of ERK1/2 Is Decreased in PCOS Theca Cells as Compared with Normal Theca Cells Irrespective of the Insulin Concentration

Fourth-passage theca cells propagated from normal and PCOS patients were grown to confluent, transferred into serum-free medium without insulin for 24 h, and then treated with serum-free medium with vehicle (C) or 7.5 μM forskolin (F), without or with 2 or 20 nM insulin. Twenty-four hours thereafter, the cells were harvested, and immunoblot analysis was performed using 35 μg of whole cell extract and antibodies specific for phosphorylated ERK1/2 (Phospho-ERK1/2) and total ERK1/2. Representative immunoblot data of whole cell extracts prepared from theca cells isolated from normal and PCOS patients. Insulin treatment did not significantly affect the phosphorylation state of ERK1/2 in normal or PCOS theca cells.

cells, experiments were performed to assess the effects of insulin on ERK phosphorylation and overall androgen biosynthesis. In these experiments, theca cells propagated from multiple normal and PCOS patients were grown to subconfluent, and transferred into serum-free medium without insulin for 24 h, then treated for an additional 24 h with serum-free medium, with and without 2 or 20 nM insulin, in the presence and absence of 7.5 μM forskolin. An insulin concentration of 2 nM (*i.e.* 10 ng/ml) is equivalent to the normal plasma concentration of insulin. As shown in Fig. 7, insulin treatment did not significantly affect the phosphorylation state of ERK1/2 in normal or PCOS theca cells. ERK1/2 phosphorylation was decreased in PCOS theca cells as compared with normal theca cells, at both concentrations of insulin tested, and in the absence of insulin. In agreement with the data presented in Fig. 2, treatment with 7.5 μM forskolin reduced ERK phosphorylation approximately 50% in both normal and PCOS theca cells in the absence and presence of insulin. Of significant interest is the observation that in the absence of insulin treatment, CYP17 mRNA abundance (Fig. 8, *middle panel*), DHEA accumulation (Fig. 8, *lower panel*), and 17α-hydroxylase enzyme activity (data not shown) were increased in PCOS theca cells as compared with normal theca cells. These data suggest that alterations in MEK/ERK signaling, CYP17 mRNA accumulation, and androgen biosynthesis may not be directly associated with insulin action.

DISCUSSION

The study of human theca cells maintained in long-term culture provides an opportunity to compare the steroidogenic abnormalities and their underlying causes in PCOS theca cells (9, 10). In addition to augmented transcription of the *CYP17* gene (11, 12), recent microarray analysis of differential gene expression in normal and PCOS theca cells demonstrated that dysregulation of androgen biosynthesis is associated with selective differences in several gene networks that are involved in steroid hormone biosynthesis as well as insulin and glucose homeostasis (32–34)

In an attempt to examine the molecular mechanisms underlying dysregulated gene expression in the PCOS ovary, we have extended our studies on MAPK signaling in normal and PCOS theca cells. In this report, we present data to support the concept that increased *CYP17* gene expression and overall androgen biosynthesis are associated with diminished MEK1/2 and

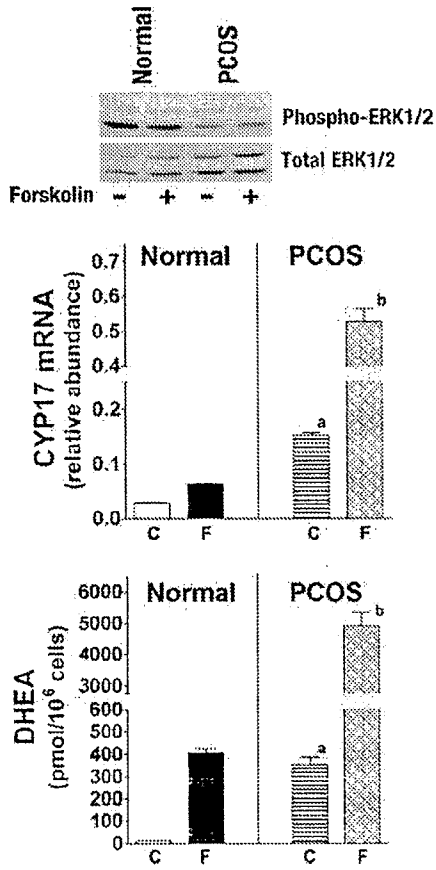

Fig. 8. CYP17 mRNA Abundance and DHEA Biosynthesis Are Increased in PCOS Theca Cells as Compared with Normal Theca Cells in the Absence of Insulin

Fourth-passage theca cells propagated from normal and PCOS patients were grown to subconfluent, transferred into serum-free medium in the absence of insulin for 24 h, and then treated with serum-free medium with vehicle (C) or 20 forskolin (F) in the absence of insulin. *Upper panel*, For analysis of ERK1/2 phosphorylation, 24 h thereafter the cells were harvested, and immunoblot analysis was performed using 35 μg of whole cell extract and antibodies specific for phosphorylated ERK1/2 (Phospho-ERK1/2) and total ERK1/2. Representative immunoblot data of whole cell extracts prepared from theca cells isolated from four independent normal and PCOS patients. *Middle panel*, At 24 h the cells were harvested and CYP17 mRNA abundance was evaluated using quantitative real-time PCR analysis. mRNA accumulation was normalized by TBP mRNA abundance and is depicted graphically as the mean ± SEM. In the absence of insulin treatment, both basal (a, $P < 0.05$) and forskolin (b, $P < 0.05$)-stimulated CYP17 mRNA accumulation were significantly increased in PCOS theca cells as compared with normal theca cells. *Bottom panel*, Seventy-two hours after treatment, the media were collected and DHEA production was evaluated by RIA. Data were normalized to cell number and are presented as the mean ± SEM from triplicate theca cell cultures from four independent normal and PCOS patients. In the absence of insulin treatment, both basal (a, $P < 0.05$) and forskolin (b, $P < 0.05$)-stimulated CYP17 mRNA accumulation were significantly increased in PCOS theca cells as compared with normal theca cells.

ERK1/2 signaling in the PCOS ovary. We compared the phosphorylation states of MEK1/2 and ERK1/2 in the same normal and PCOS theca cell preparations that we previously examined in our *CYP17* transcriptional studies (11, 12) and microarray analysis (32). The comparison of the phosphorylation states of MEK1/2 and ERK1/2 in normal and PCOS theca cells propagated in long-term culture revealed a gross reduction in the tone of MEK/ERK signaling in PCOS cells.

Infection of normal theca cells with a dominant-negative MEK1 adenovirus resulted in increased DHEA production, CYP17 mRNA accumulation, and 17α-hydroxylase enzyme activity, and treatment with the pharmacological MEK1 inhibitor, PD, augmented *CYP17* gene transcription. In contrast, infection with a constitutively active MEK1 inhibited both DHEA synthesis and CYP17 mRNA accumulation. In our comparison of *CYP17* promoter function in normal and PCOS theca cells, the observed lack of a response of PCOS theca cells to PD further supports the idea that the suppression of the MEK/ERK signaling pathway plays a pivotal role in regulating androgen synthesis in the PCOS ovary.

Although several investigators have examined the mechanisms by which insulin and IGF acutely stimulate the ERK1/2 signaling pathway in porcine and human theca cells (31, 35, 36), there is no information available with respect to the intracellular signaling pathways mediating androgen biosynthesis in normal and PCOS theca cells under basal and cAMP-stimulated conditions. In addition, most studies have focused on the acute regulation of MEK or ERK phosphorylation in response to a variety of stimuli, rather than examining MAPK signaling under steady-state conditions in differentiated cells. In contrast, we compared MAPK signaling using conditions in which normal and PCOS theca cells are fully differentiated. Data from array analysis suggests that cross talk between several signaling pathways, including the MAPK pathway, may be dysregulated in the PCOS ovary. For instance tribble 3, which inhibits Akt/protein kinase B (PKB) phosphorylation, exhibits decreased gene expression in PCOS theca cells, and cAMP-GEFII, which augments Akt/PKB phosphorylation, exhibits increased gene expression in PCOS theca cells (32).

PCOS is also associated with insulin resistance, obesity, and type II diabetes (37). Insulin resistance and hyperinsulinemia in PCOS have been hypothesized to contribute to increased androgen production by the ovary. Although several investigators had initially proposed that hyperinsulinemia, resulting from the insulin-resistant state, produces ovarian hyperandrogenism by spillover occupancy and activation of the IGF-I receptors (38), the studies of Nestler *et al.* (6) have conclusively demonstrated that PCOS theca cells are not insulin resistant and are responsive to insulin. However, there are no apparent differences in insulin sensitivity between normal and PCOS theca cells, and insulin appears to act via its own receptor rather than through spillover occupancy of the IGF-I

receptor (6). No differences were found in the ED_{50} of insulin-stimulated steroid biosynthesis in freshly isolated granulosa cells (39, 40) obtained from normal and PCOS ovaries. These data are in agreement with our data demonstrating that insulin treatment does not differentially affect ERK1/2 phosphorylation in normal or PCOS theca cells. Furthermore, in the absence of insulin, CYP17 mRNA abundance and DHEA accumulation was increased in PCOS theca cells as compared with normal theca cells, and the phosphorylation state of ERK1/2 was decreased in PCOS theca cells, as compared with normal theca cells.

In human adrenal cells, Sewer *et al.* (41) has established that there is cross talk between the MAPK and ACTH/cAMP pathways in the regulation of CYP17 mRNA synthesis. These authors demonstrated that a reduction in the activation state of the ERK1/2 is associated with increased *CYP17* gene expression in adrenal cells (41). These authors also showed that protein kinase A phosphorylates and activates a dual-specificity phosphatase, MAPK phosphatase-1 (MKP-1), which mediates *CYP17* gene transcription in response to ACTH/cAMP (28, 41). However, these investigators did not report the role of ERK1/2 or MKP-1 in overall adrenal androgen biosynthesis. Therefore, the possible involvement of MKP-1 in augmented *CYP17* gene expression and increased androgen biosynthesis in normal and PCOS theca cells is unclear and will require future examination.

We are in the process of examining the relationship between the cohort of multiple signaling pathways and transcription factors that confer increased *CYP17* gene expression in PCOS theca cells. The reduction in MEK1/2 and ERK1/2 phosphorylation in PCOS cells is also in agreement with our previously published data demonstrating that a relief of transcriptional repression may play a role in augmented transcriptional regulation of the *CYP17* gene in the PCOS ovary (11). Analysis of the *CYP17* promoter function in normal and PCOS theca cells demonstrated that a 16-bp sequence, spanning −174 to −158 bp of the *CYP17* promoter confers increased expression of the *CYP17* promoter in PCOS theca cells (11). We reported that transcription factor, NF-1 C, bound to this element and was able to repress *CYP17* promoter function (11). Identification of the cohort of transcription factors that regulate this element will further our knowledge of the underlying cause(s) of increased *CYP17* gene expression in PCOS theca cells and the extent to which defects in MAPK signaling and other signaling pathways are involved in the pathogenesis of PCOS.

In patients with insulin resistance and type II diabetes, there are reports of alterations in multiple components of the phosphoinositol 3-kinase/PKB and Ras/MAPK signaling pathways (42–51). Yet, there are very few reports of the specific signaling defects observed in PCOS patients. In patients with PCOS and insulin resistance, there are reports to suggest that D-chiro-inositol signaling is altered (6, 52–55). Dunaif *et al.* and Li *et al.* (56, 57) have reported that insulin receptor autophosphorylation is decreased in fibroblasts in approximately 50% of patients with PCOS. Whereas in PCOS adipocytes, Ciaraldi *et al.* (58, 59) reported that insulin resistance is accompanied by normal function of the insulin receptor, but involves a novel postreceptor defect in the insulin signal transduction between the receptor kinase and glucose transport. With respect to the ovary, although it is well recognized that LH-, FSH-, and insulin receptor sensitivity are increased in ovarian cells isolated from PCOS patients (5, 38–40, 60–62), there are few data that describe defects in cellular signaling in PCOS ovarian cells other than those demonstrating decreased abundance of insulin receptor substrate-2 mRNA and protein in PCOS granulosa and theca cells (63).

The data presented in this report are the first to suggest that MAPK signaling in normal and PCOS cells is distinct. These studies have demonstrated that decreased MEK/ERK phosphorylation are directly associated with increased thecal *CYP17* gene expression and androgen biosynthesis. Moreover, our findings reveal that in the absence of insulin treatment, phosphorylation state of ERK1/2 is decreased, and CYP17 mRNA accumulation and DHEA biosynthesis are increased in PCOS cells as compared with normal cells. We are currently characterizing the extent to which other components of the MAPK signaling pathway regulate increased *CYP17* gene expression and androgen excess in the PCOS ovary. As a consequence of future studies we hope to further our understanding of the underlying cause of increased *CYP17* gene expression and possibly other abnormalities in PCOS, *e.g.* insulin resistance, obesity, arrested follicular development, and endometrial cancer.

MATERIALS AND METHODS

Theca Cell Isolation and Propagation

Human theca interna tissue was obtained from follicles of women undergoing hysterectomy, under a protocol approved by the Institutional Review Board of the Pennsylvania State University College of Medicine. Individual follicles were dissected away from ovarian stroma. The isolated follicles were size selected for diameters ranging from 3–5 mm so that theca cells derived from follicles of similar size from normal and PCOS subjects could be compared. The dissected follicles were placed into serum-containing medium and bisected. Under a dissecting microscope, the theca interna was stripped from the follicle wall, and the granulosa cells were removed with a platinum loop. The cleaned theca shells were dispersed with 0.05% collagenase I, 0.05% collagenase IA, and 0.01% deoxyribonuclease, in medium containing 10% fetal bovine serum (FBS) (64). Dispersed cells were placed in culture dishes that had been precoated with fibronectin by incubation at 37 C with culture medium containing 5 μg/ml human fibronectin. The growth medium used was a 1:1 mixture of DMEM and Hams F-12 medium containing 10% FBS, 10% horse serum, 2% UltroSer G, 20 nM insulin, 20 nM selenium, 1 μM vitamin E, and antibiotics. From each follicle, twelve 35-mm dishes of primary theca interna cells were grown until confluent, removed from the dish with neutral protease (pronase-E; protease type XXIV, Sigma, St.

Louis, MO) in DMEM/F12 (1:1), frozen, and stored in liquid nitrogen (one 35-mm dish per vial) in culture medium that contained 20% FBS and 10% dimethylsulfoxide. In all experiments, cells were thawed and propagated in the growth medium described above. To obtain successive passages of normal and PCOS theca cells, cells were thawed, propagated, and frozen at consecutive passages. The cells were grown in 5% O_2, 90% N_2, and 5% CO_2. Reduced oxygen tension and supplemental antioxidants (vitamin E and selenium) were employed to prevent oxidative damage.

The PCOS and normal ovarian tissue came from age-matched women, 38–40 yr old. The diagnosis of PCOS was made according to established guidelines (2, 65–67), including hyperandrogenemia, oligoovulation, and the exclusion of 21α-hydroxylase deficiency, Cushing's syndrome, and hyperprolactinemia. All of the PCOS theca cell preparations studied came from ovaries of women with fewer than six menses per year and elevated serum total testosterone or bioavailable testosterone levels, as previously described (2, 9). Each of the PCOS ovaries contained multiple subcortical follicles of less than 10 mm in diameter. The control (normal) theca cell preparations came from ovaries of fertile women with normal menstrual histories, menstrual cycles of 21–35 d, and no clinical signs of hyperandrogenism. Neither PCOS nor normal subjects were receiving hormonal medications at the time of surgery. Indications for surgery were dysfunctional uterine bleeding, endometrial cancer, and pelvic pain. The passage conditions and split ratios for all normal and PCOS cells were identical. Experiments comparing PCOS and normal theca were performed using fourth-passage (31–38 population doublings) theca cells isolated from size-matched follicles obtained from age-matched subjects. Sera and growth factors were obtained from the following sources: FBS and DMEM/F12 were obtained from Irvine Scientific (Irvine, CA); horse serum was obtained from Hyclone (Logan, UT); UltroSer G was from Reactifs IBF (Villeneuve-la-Garenne, France). Other compounds were purchased from Sigma.

Western Blot Analysis

Fourth-passage normal and PCOS theca cells were grown until subconfluent and transferred into serum-free medium with and without forskolin for 24 h. After treatment, theca cells were harvested in ice cold modified RIPA buffer (30 mM Tris, 150 mM NaCl, 50 mM Na F, 0.5 mM EDTA, 0.5% deoxycholic acid, 1.0% Nonidet P-40, 0.1% sodium dodecyl sulfate) containing 1 mM sodium orthovanadate, 0.1 mM phenymethylsufonyl fluoride, 1 mM dithiothreitol, 0.2 mM benzamidine, 1 μM microcystin, 1 μg/ml leupeptin, and 1 μg/ml pepstatin A. Protein concentration was determined using a bicinchoninic acid protein assay (Pierce, Rockford, IL). Whole cell lysates (35 μg/lane) were separated on a 10% SDS-PAGE, transferred to polyvinylidene difluoride membrane, and Western analysis was performed as previously described (68). Total and phosphospecific MEK1/2 and ERK1/2 used in Western analysis were obtained from Cell Signaling Technology (Beverly, MA).

Replication-Deficient Adenovirus Infections

Adenoviruses expressing constitutively active MEK1 (Ser218 and Ser222 to Glu, CA-MEK1), and/or dominant-negative MEK1 (Ser222 to Ala, DN-MEK1) were used as previously described (29, 30, 69). All recombinant adenoviral vectors were plaque purified, expanded, and titered by detection of formation of visible plaques in a HEK293 monolayer of cells using the agarose gel overlay method. Adenoviral infections involved growing fourth-passage theca cells to 95% confluence, rinsing the cells with PBS, and layering of the adenovirus on the cells in 50% of the normal treatment volume of serum-free medium for 1 h. Subsequently, the cells were cultured in serum-free media with and without treatment as indicated. Using these conditions, >98% of cells showed positive β-Gal staining after infection with the LacZ adenovirus.

Steroid Biosynthesis

For evaluation of steroid production, theca cells were grown until subconfluent and transferred into serum-free medium in the presence or absence of forskolin (20 μM) with and without varying concentrations of adenovirus. At 72 h, the media was collected and RIAs for DHEA were performed without organic solvent extraction using Diagnostic Products (Los Angeles, CA) as previously described (68).

Quantitation of CYP17 mRNA

For quantitative real-time PCR, total mRNA was isolated (9) from fourth-passage theca cells that were grown to subconfluence, transferred into serum-free medium, and treated as indicated. RNA (1 μg) samples were then reverse transcribed using oligo deoxythymidine and 200 units Stratascript Reverse Transcriptase (Stratagene, Cedar Creek, TX), and CYP17 mRNA abundance was determined by quantitative real-time PCR as previously described (68). The gene-specific two-step PCR was carried out in triplicate for each cDNA sample and for a series of serial dilutions in an Mx4000 Thermocycler (Stratagene, Cedar Creek, TX) using the Mx4000 Multiplex Quantitative PCR system according to manufacturer's instructions. TATA-box binding protein (TBP) mRNA abundance was used for data normalization.

17α-Hydroxylase Enzyme Activity

For evaluation of 17α-hydroxylase enzyme activity, normal theca cells were grown until subconfluent, then infected with adenovirus and transferred to serum-free medium and treated as indicated for 72 h. The cells were then transferred into medium containing a saturating concentration of 1.0 μM [1,2,6,7-^{3}H]progesterone and the rate of conversion to 17α-hydroxyprogesterone and 17α, 20α-dihydroprogesterone was determined as we have previously reported (9, 10). Cell number was estimated using a Coulter counter (Coulter Electronics, Hialeah, FL) after dispersal of cells with trypsin. Steroidogenic enzyme activities are expressed as picomoles per 10^6 cells/hour.

Transient Transfection Assay

Subconfluent cultures of theca cells were transfected with reporter gene constructs as we have previously described (11, 12) using the modified calcium-phosphate method of Graham and Vander Eb (70). One hour before transfection, the cells were transferred into DMEM high-glucose medium containing 20 mM HEPES and 2% heat inactivated calf serum, and moved to a 3% CO_2, 95% ambient air 37 C incubator. DNA/Ca2P04 solution containing 20 μg of reporter plasmid, and 1 μg of pSV-β-Gal/100-mm dish in HEPES phosphate buffer was added to the media. After incubation for 6 h, cells were transferred into 2% calf serum in DMEM containing 20 mM HEPES and treated as described. Seventy-two hours after forskolin treatment, the cells were harvested using trypsin/EDTA, pelleted, and resuspended in reporter lysis buffer for LUC assays. LUC assays were performed using the LUC assay system (Promega, Madison, WI). β-Gal activities were determined by Galacton Light Plus chemiluminescent assay (Tropix, Bedford, MA) and used to normalize LUC activities.

Statistical Analysis

Each experiment was performed using triplicate dishes. After combining the results from individual experiments, nonparametric Mann Whitney tests were performed using PRISM 4.0 from SAS Institute, Inc. (Cary, NC). $P < 0.05$ was considered statistically significant.

Acknowledgments

We thank Dr. Jeffery D. Molkentin (Department of Pediatrics, Children's Hospital Medical Center, University of Cincinnati, Cincinnati, OH) for providing adenoviruses encoding constitutively active and dominant-negative MEK1. We are indebted to Dr. David Spector (Department of Microbiology, Pennsylvania State College of Medicine, Hershey, PA) for his expertise in adenoviral propagation, purification, and plaque titration.

Received April 28, 2004. Accepted October 20, 2004.

Address all correspondence and requests for reprints to: Jan M. McAllister, Department of Cellular and Molecular Physiology, Pennsylvania State University College of Medicine 500 University Drive H166, Hershey, Pennsylvania 17033. E-mail: jmcallister@psu.edu.

This work was supported by National Institutes of Health Grants HD33852 (to J.M.M. and R.S.L.), HD34449 (to J.M.M., R.S.L., and J.F.S.).

REFERENCES

1. Franks S, Gharani N, Waterworth D, Batty S, White D, Williamson R, McCarthy M 1997 The genetic basis of polycystic ovary syndrome. Hum Reprod 12:2641–2648
2. Legro R, Driscoll D, Strauss III J, Fox A, Dunaif A 1998 Evidence for a genetic basis for hyperandrogenemia in polycystic ovary syndrome. Proc Natl Acad Sci USA 95: 14956–14960
3. Strauss 3rd JF 2003 Some new thoughts on the pathophysiology and genetics of polycystic ovary syndrome. Ann NY Acad Sci 997:42–48
4. Jakubowicz D, Nestler J 1997 17α-Hydroxyprogesterone response to leuprolide and serum androgens in PD treatment was observed to inhibit ERK1/2 phosphorylation in normal theca cells to a greater extent than in PCOS theca cells obese women with and without polycystic ovary syndrome after dietary weight loss. J Clin Endocrinol Metab 82:556–559
5. Gilling-Smith C, Story H, Rogers V, Franks S 1997 Evidence for a primary abnormality in theca cell steroidogenesis in the polycystic ovarian syndrome. Clin Endocrinol (Oxf) 47:1158–1165
6. Nestler JE, Jakubowicz DJ, de Vargas AF, Brik C, Quintero N, Medina F 1998 Insulin stimulates testosterone biosynthesis by human thecal cells from women with polycystic ovary syndrome by activating its own receptor and using inositolglycan mediators as the signal transduction system. J Clin Endocrinol Metab 83:2001–2005
7. Voutilainen R, Tapanainen J, Chung BC, Matteson KJ, Miller WL 1986 Hormonal regulation of P450scc (20,22-desmolase) and P450c17 (17α-hydroxylase/17,20-lyase) in cultured human granulosa cells. J Clin Endocrinol Metab 63:202–207
8. McAllister J, Kerin J, Trant J, Estabrook R, Mason J, Waterman M, Simpson E 1989 Regulation of cholesterol side-chain cleavage and 17α-hydroxylase/lyase activities in proliferating theca interna cells in long term monolayer culture. Endocrinology 125:1959–1966
9. Nelson V, Legro R, Strauss J, McAllister J 1999 Augmented androgen production is a stable phenotype of propagated theca cells from polycystic ovaries. Mol Endocrinol 13:946–957
10. Nelson VL, Qin Kn KN, Rosenfield RL, Wood JR, Penning TM, Legro RS, Strauss 3rd JF, McAllister JM 2001 The biochemical basis for increased testosterone production in theca cells propagated from patients with polycystic ovary syndrome. J Clin Endocrinol Metab 86:5925–5933
11. Wickenheisser JK, Nelson-DeGrave VL, Quinn PG, McAllister JM 2004 Increased cytochrome P450 17α-hydroxylase promoter function in theca cells isolated from patients with polycystic ovary syndrome involves nuclear factor-1. Mol Endocrinol 18:588–605
12. Wickenheisser JK, Quinn PG, Nelson VL, Legro RS, Strauss JF, McAllister JM 2000 Differential activity of the cytochrome P450 17α-hydroxylase and steroidogenic acute regulatory protein gene promoters in normal and polycystic ovary syndrome theca cells. J Clin Endocrinol Metab 85:2304–2311
13. Carvalho CR, Carvalheira JB, Lima MH, Zimmerman SF, Caperuto LC, Amanso A, Gasparetti AL, Meneghetti V, Zimmerman LF, Velloso LA, Saad MJ 2003 Novel signal transduction pathway for luteinizing hormone and its interaction with insulin: activation of Janus kinase/signal transducer and activator of transcription and phosphoinositol 3-kinase/Akt pathways. Endocrinology 144: 638–647
14. Salvador LM, Park Y, Cottom J, Maizels ET, Jones JC, Schillace RV, Carr DW, Cheung P, Allis CD, Jameson JL, Hunzicker-Dunn M 2001 Follicle-stimulating hormone stimulates protein kinase A-mediated histone H3 phosphorylation and acetylation leading to select gene activation in ovarian granulosa cells. J Biol Chem 276: 40146–40155
15. Das S, Maizels ET, DeManno D, St Clair E, Adam SA, Hunzicker-Dunn M 1996 A stimulatory role of cyclic adenosine 3′,5′-monophosphate in follicle-stimulating hormone-activated mitogen-activated protein kinase signaling pathway in rat ovarian granulosa cells. Endocrinology 137:967–974
16. Tajima K, Dantes A, Yao Z, Sorokina K, Kotsuji F, Seger R, Amsterdam A 2003 Down-regulation of steroidogenic response to gonadotropins in human and rat preovulatory granulosa cells involves mitogen-activated protein kinase activation and modulation of DAX-1 and steroidogenic factor-1. J Clin Endocrinol Metab 88:2288–2299
17. Whitmarsh A, Davis R 1996 Transcription factor AP-1 regulation by mitogen-activated protein kinase signal transduction pathways. J Mol Med 74:589–607
18. Vossler M, Yao H, York R, Pan M, Rim C, Stork P 1997 cAMP activates MAP kinase and ELK-1 through a B-Raf- and Rap1-dependent pathway. Cell 89:73–82
19. Widmann C, Gibson S, Jarpe M, Johnson G 1999 Mitogen-activated protein kinase: conservation of a three-kinase module from yeast to human. Physiol Rev 79: 143–180
20. Mulder K 2000 Role of Ras and Mapks in TGFβ signaling. Cytokine Growth Factor Rev 11:23–25
21. Yang SH, Sharrocks AD, Whitmarsh AJ 2003 Transcriptional regulation by the MAP kinase signaling cascades. Gene 320:3–21
22. Pestell RG, Albanese C, Watanabe G, Johnson J, Eklund N, Lastowiecki P, Jameson JL 1995 Epidermal growth factor and c-Jun act via a common DNA regulatory element to stimulate transcription of the ovine P-450 cholesterol side chain cleavage (CYP11A1) promoter. J Biol Chem 270:18301–18308
23. Price M, Rogers A, Treisman R 1995 Comparative analysis of the ternary complex factors Elk-1, SAP-1a and SAP-2 (ERP/NET). EMBO J 14:2589–2601
24. Dudley DT, Pang L, Decker SJ, Bridges AJ, Saltiel AR 1995 A synthetic inhibitor of the mitogen-activated pro-

tein kinase cascade. Proc Natl Acad Sci USA 92: 7686–7689
25. Favata MF, Horiuchi KY, Manos EJ, Daulerio AJ, Stradley DA, Feeser WS, Van Dyk DE, Pitts WJ, Earl RA, Hobbs F, Copeland RA, Magolda RL, Scherle PA, Trzaskos JM 1998 Identification of a novel inhibitor of mitogen-activated protein kinase kinase. J Biol Chem 273: 18623–18632
26. Gyles SL, Burns CJ, Whitehouse BJ, Sugden D, Marsh PJ, Persaud SJ, Jones PM 2001 ERKs regulate cyclic AMP-induced steroid synthesis through transcription of the steroidogenic acute regulatory (StAR) gene. J Biol Chem 276:34888–34895
27. Sewer MB, Waterman MR 2002 Adrenocorticotropin/cyclic adenosine 3′,5′-monophosphate-mediated transcription of the human CYP17 gene in the adrenal cortex is dependent on phosphatase activity. Endocrinology 143:1769–1777
28. Sewer MB, Waterman MR 2002 cAMP-dependent transcription of steroidogenic genes in the human adrenal cortex requires a dual-specificity phosphatase in addition to protein kinase A. J Mol Endocrinol 29:163–174
29. Liang Q, Wiese RJ, Bueno OF, Dai YS, Markham BE, Molkentin JD 2001 The transcription factor GATA4 is activated by extracellular signal-regulated kinase 1- and 2-mediated phosphorylation of serine 105 in cardiomyocytes. Mol Cell Biol 21:7460–7469
30. Fujishiro M, Gotoh Y, Katagiri H, Sakoda H, Ogihara T, Anai M, Onishi Y, Ono H, Funaki M, Inukai K, Fukushima Y, Kikuchi M, Oka Y, Asano T 2001 MKK6/3 and p38 MAPK pathway activation is not necessary for insulin-induced glucose uptake but regulates glucose transporter expression. J Biol Chem 276:19800–19806
31. Munir I, Yen HW, Geller DH, Torbati D, Bierden RM, Weitsman SR, Agarwal SK, Magoffin DA 2004 Insulin augmentation of 17α-hydroxylase activity is mediated by phosphatidyl inositol 3-kinase but not extracellular signal-regulated kinase-1/2 in human ovarian theca cells. Endocrinology 145:175–183
32. Wood JR, Nelson VL, Ho C, Jansen E, Wang CY, Urbanek M, McAllister JM, Mosselman S, Strauss 3rd JF 2003 The molecular phenotype of polycystic ovary syndrome (PCOS) theca cells and new candidate PCOS genes defined by microarray analysis. J Biol Chem 278: 26380–26390
33. Legro RS 2000 The genetics of obesity. Lessons for polycystic ovary syndrome. Ann NY Acad Sci 900: 193–202
34. Daneshmand S, Weitsman SR, Navab A, Jakimiuk AJ, Magoffin DA 2002 Overexpression of theca-cell messenger RNA in polycystic ovary syndrome does not correlate with polymorphisms in the cholesterol side-chain cleavage and 17α-hydroxylase/C(17–20) lyase promoters. Fertil Steril 77:274–280
35. Zhang G, Veldhuis JD 2004 Insulin drives transcriptional activity of the CYP17 gene in primary cultures of swine theca cells. Biol Reprod 70:1600–1605
36. Veldhuis JD, Zhang G, Garmey JC 2002 Troglitazone, an insulin-sensitizing thiazolidinedione, represses combined stimulation by LH and insulin of de novo androgen biosynthesis by thecal cells *in vitro*. J Clin Endocrinol Metab 87:1129–1133
37. Dunaif A 1999 Insulin action in the polycystic ovary syndrome. Endocrinol Metab Clin North Am 28:341–359
38. Barbieri R, Makis A, Randall R, Daniels G, Kristner R, Ryan K 1986 Insulin stimulates androgen accumulation in incubations of ovarian stroma obtained from women with hyperandrogenism. J Clin Endocrinol Metab 62:904–910
39. Willis D, Mason H, Gilling-Smith C, Franks S 1996 Modulation by insulin of follicle-stimulating hormone and luteinizing hormone actions in human granulosa cells of normal and polycystic ovaries. J Clin Endocrinol Metab 81:302–309
40. Willis D, Franks S 1995 Insulin action in human granulosa cells from normal and polycystic ovaries is mediated by the insulin receptor and not the type-I insulin-like growth factor receptor. J Clin Endocrinol Metab 80:3788–3790
41. Sewer MB, Waterman MR 2003 cAMP-dependent protein kinase enhances CYP17 transcription via MKP-1 activation in H295R human adrenocortical cells. J Biol Chem 278:8106–8111
42. Kruszynska YT, Olefsky JM 1996 Cellular and molecular mechanisms of non-insulin dependent diabetes mellitus. J Invest Med 44:413–428
43. Hall RK, Granner DK 1999 Insulin regulates expression of metabolic genes through divergent signaling pathways. J Basic Clin Physiol Pharmacol 10:119–133
44. Jones DR, Varela-Nieto I 1999 Diabetes and the role of inositol-containing lipids in insulin signaling. Mol Med 5:505–514
45. Smith U, Axelsen M, Carvalho E, Eliasson B, Jansson PA, Wesslau C 1999 Insulin signaling and action in fat cells: associations with insulin resistance and type 2 diabetes. Ann NY Acad Sci 892:119–126
46. Begum N, Ragolia L 1998 Altered regulation of insulin signaling components in adipocytes of insulin-resistant type II diabetic Goto-Kakizaki rats. Metabolism 47:54–62
47. Cusi K, Maezono K, Osman A, Pendergrass M, Patti ME, Pratipanawatr T, DeFronzo RA, Kahn CR, Mandarino LJ 2000 Insulin resistance differentially affects the PI 3-kinase- and MAP kinase-mediated signaling in human muscle. J Clin Invest 105:311–320
48. Grzelkowska K, Dardevet D, Balage M, Grizard J 1999 Involvement of the rapamycin-sensitive pathway in the insulin regulation of muscle protein synthesis in streptozotocin-diabetic rats. J Endocrinol 160:137–145
49. Kahn CR, Vicent D, Doria A 1996 Genetics of non-insulin-dependent (type-II) diabetes mellitus. Annu Rev Med 47: 509–531
50. Reynet C, Kahn CR 1993 Rad: a member of the Ras family overexpressed in muscle of type II diabetic humans. Science 262:1441–1444
51. Knebel B, Kotzka J, Avci H, Schiller M, Bruning JC, Hafner M, Krone W, Muller-Wieland D 2000 Characterization of a postreceptor signaling defect that impairs cfos expression in cultured fibroblasts of a patient with insulin resistance. Biochem Biophys Res 268:577–582
52. Asplin I, Galasko G, Larner J 1993 Chiro-inositol deficiency and insulin resistance: a comparison of the chiro-inositol- and the myo-inositol-containing insulin mediators isolated from urine, hemodialysate, and muscle of control and type II diabetic subjects. Proc Natl Acad Sci USA 90:5924–5928
53. Larner J, Allan G, Kessler C, Reamer P, Gunn R, Huang LC 1998 Phosphoinositol glycan derived mediators and insulin resistance. Prospects for diagnosis and therapy. J Basic Clin Physiol Pharmacol 9:127–137
54. Nestler JE, Jakubowicz DJ, Reamer P, Gunn RD, Allan G 1999 Ovulatory and metabolic effects of D-*chiro*-inositol in the polycystic ovary syndrome. N Engl J Med 340: 1314–1320
55. Baillargeon JP, Iuorno MJ, Jakubowicz DJ, Apridonidze T, He N, Nestler JE 2004 Metformin therapy increases insulin-stimulated release of D-*chiro*-inositol-containing inositolphosphoglycan mediator in women with polycystic ovary syndrome. J Clin Endocrinol Metab 89:242–249
56. Dunaif A, Xia J, Book CB, Schenker E, Tang Z 1995 Excessive insulin receptor serine phosphorylation in cultured fibroblasts and in skeletal muscle. A potential mechanism for insulin resistance in the polycystic ovary syndrome. J Clin Invest 96:801–810
57. Li M, Youngren JF, Dunaif A, Goldfine ID, Maddux BA, Zhang BB, Evans JL 2002 Decreased insulin receptor (IR) autophosphorylation in fibroblasts from patients with PCOS: effects of serine kinase inhibitors and IR activators. J Clin Endocrinol Metab 87:4088–4093

58. Ciaraldi TP, el-Roeiy A, Madar Z, Reichart D, Olefsky JM, Yen SS 1992 Cellular mechanisms of insulin resistance in polycystic ovarian syndrome. J Clin Endocrinol Metab 75:577–583
59. Ciaraldi TP 2000 Molecular defects of insulin action in the polycystic ovary syndrome: possible tissue specificity. J Pediatr Endocrinol Metab 13(Suppl 5):1291–1293
60. Coffler MS, Patel K, Dahan MH, Malcom PJ, Kawashima T, Deutsch R, Chang RJ 2003 Evidence for abnormal granulosa cell responsiveness to follicle-stimulating hormone in women with polycystic ovary syndrome. J Clin Endocrinol Metab 88:1742–1747
61. Coffler MS, Patel K, Dahan MH, Yoo RY, Malcom PJ, Chang RJ 2003 Enhanced granulosa cell responsiveness to follicle-stimulating hormone during insulin infusion in women with polycystic ovary syndrome treated with pioglitazone. J Clin Endocrinol Metab 88:5624–5631
62. Gilling-Smith C, Willis DS, Beard RW, Franks S 1994 Hypersecretion of androstenedione by isolated thecal cells from polycystic ovaries. J Clin Endocrinol Metab 79:1158–1165
63. Wu XK, Zhou SY, Liu JX, Pollanen P, Sallinen K, Makinen M, Erkkola R 2003 Selective ovary resistance to insulin signaling in women with polycystic ovary syndrome. Fertil Steril 80:954–965
64. McAllister J, Simpson E 1993 Human theca interna cells in culture. San Diego: Academic Press
65. The Rotterdam ESHRE/ASRM Sponsored Group 2004 Revised 2003 consensus on diagnostic criteria and long-term health risks related to polycystic ovary syndrome (PCOS). Hum Reprod 19:41–47
66. Zawadzki J, Dunaif A 1992 Diagnostic criteria for polycystic ovary syndrome: towards a rational approach. Boston: Blackwell Scientific Publications
67. Legro RS 2003 Diagnostic criteria in polycystic ovary syndrome. Semin Reprod Med 21:267–275
68. Nelson-DeGrave VL, Wickenheisser JK, Cockrell JE, Wood JR, Legro RS, Strauss 3rd JF, McAllister JM 2004 Valproate potentiates androgen biosynthesis in human ovarian theca cells. Endocrinology 145: 799–808
69. De Windt LJ, Lim HW, Haq S, Force T, Molkentin JD 2000 Calcineurin promotes protein kinase C and c-Jun NH2-terminal kinase activation in the heart. Cross-talk between cardiac hypertrophic signaling pathways. J Biol Chem 275:13571–13579
70. Graham F, van der Eb A 1973 A new technique for the assay of infectivity of human adenovirus 5 DNA. Virology 52:456–457

Molecular Endocrinology **is published monthly by The Endocrine Society (http://www.endo-society.org), the foremost professional society serving the endocrine community.**

Diabetologia (2005) 48: 336–344
DOI 10.1007/s00125-004-1636-8

ARTICLE

T. Sasaoka · K. Fukui · T. Wada · S. Murakami · J. Kawahara · H. Ishihara · M. Funaki · T. Asano · M. Kobayashi

Inhibition of endogenous SHIP2 ameliorates insulin resistance caused by chronic insulin treatment in 3T3-L1 adipocytes

Received: 28 April 2004 / Accepted: 4 September 2004 / Published online: 15 January 2005

Abstract *Aims/hypothesis:* SHIP2 is a physiologically important negative regulator of insulin signalling hydrolysing the PI3-kinase product, PI(3,4,5)P3, which also has an impact on insulin resistance. In the present study, we examined the effect of inhibiting the endogenous SHIP2 function on the insulin resistance caused by chronic insulin treatment. *Methods:* The endogenous function of SHIP2 was inhibited by expressing a catalytically inactive SHIP2 (ΔIP-SHIP), and compared with the effect of treatments designed to restore the levels of IRS-1 in insulin signalling systems of 3T3-L1 adipocytes. *Results:* Chronic insulin treatment induced the large (86%) down-regulation of IRS-1 and the modest (36%) up-regulation of SHIP2. Subsequent stimulation by insulin of Akt phosphorylation, PKCλ activity, and 2-deoxyglucose (2-DOG) uptake was markedly decreased by the chronic insulin treatment. Coincubation with the mTOR inhibitor, rapamycin, effectively inhibited the proteosomal degradation of IRS-1 caused by the chronic insulin treatment. Although the coincubation with rapamycin and advanced overexpression of IRS-1 effectively ameliorated subsequent insulin-induced phosphorylation of Akt, insulin stimulation of PKCλ activity and 2-DOG uptake was partly restored by these treatments. Similarly, expression of ΔIP-SHIP2 effectively ameliorated the insulin-induced phosphorylation of Akt without affecting the amount of IRS-1. Furthermore, the decreased insulin-induced PKCλ activity and 2-DOG uptake following chronic insulin treatment were ameliorated by the expression of ΔIP-SHIP2 more effectively than by the treatment with rapamycin. *Conclusions/interpretation:* Our results indicate that the inhibition of endogenous SHIP2 is effective in improving the state of insulin resistance caused by chronic insulin treatment.

Keywords Akt · Glucose uptake · Insulin · Insulin resistance · PKCλ · SHIP2

Abbreviations 2-DOG: 2-deoxyglucose · Glut4: glucose transporter 4 · IRS-1: insulin receptor substrate-1 · mTOR: mammalian target of rapamycin · PDGF: platelet-derived growth factor · PI3-kinase: phosphatidylinositol 3-kinase · PI(3,4)P2: phosphatidylinositol 3,4-bisphosphate · PI(3,4,5)P3: phosphatidylinositol 3,4,5-triphosphate · PKC: protein kinase C · SHIP2: SH2-containing inositol 5′-phosphatase 2

T. Sasaoka (✉)
Department of Clinical Pharmacology, Toyama Medical and Pharmaceutical University,
2630 Sugitani,
Toyama, 930-0194, Japan
e-mail: tsasaoka-tym@umin.ac.jp
Tel.: +81-76-4347551
Fax: +81-76-4345067

K. Fukui · T. Wada · S. Murakami · J. Kawahara · M. Kobayashi
First Department of Internal Medicine, Toyama Medical and Pharmaceutical University,
2630 Sugitani,
Toyama, 930-0194, Japan

H. Ishihara
Sainou Hospital,
Toyama, 930-0887, Japan

M. Funaki · T. Asano
Department of Internal Medicine, Graduate School of Medicine, University of Tokyo,
Tokyo, 113-8655, Japan

Introduction

The activation of phosphatidylinositol 3-kinase (PI3-kinase) is known to be important to the various metabolic actions of insulin [1–4]. PI(3,4,5)P3 produced by activated PI3-kinase is thought to function as a key lipid second messenger in insulin signalling to further downstream molecules [3–5]. We and others identified SH2-containing inositol 5′-phosphatase 2 (SHIP2) as a lipid phosphatase possessing 5′-phosphatase activity to hydrolyse PI(3,4,5)P3 to PI(3,4)P2 [6, 7]. Previous reports have indicated that overexpression of SHIP2 inhibits insulin-induced glucose uptake and glycogen synthesis via its 5′-phosphatase activity in 3T3-L1 adipocytes and L6 myocytes [8, 9]. Targeted

disruption of the SHIP2 gene in mice increased sensitivity to insulin without affecting other biological systems [10]. These findings indicate that SHIP2 is a physiologically important negative regulator that is relatively specific to insulin signalling. In addition, expression of SHIP2 protein is enhanced in the skeletal muscle and fat tissue of diabetic db/db mice [11]. Treatment with the insulin-senzsitizing thiazolidinedione, rosiglitazone, lowered the elevated levels of SHIP2 in the db/db mice [11]. Furthermore, a deletion in the 3′ untranslated region within the motifs implicated in the control of protein synthesis leading to the possible increase in expression of SHIP2 protein was identified in the UK and Belgian population of individuals with type 2 diabetes [12]. Therefore, SHIP2 is implicated in insulin resistance as a cause of type 2 diabetes in addition to the physiological importance in insulin signalling. Based on these findings, inhibition of endogenous SHIP2 function may be a target for ameliorating insulin signalling in the state of insulin resistance.

Hyperinsulinaemia is a hallmark of insulin resistance [13–15]. Chronic hyperinsulinaemia causes a desensitization to subsequent insulin responses, which appears to be part of the vicious cycle involved in the pathogenesis of type 2 diabetes [16–18]. In this regard, chronic treatment with insulin is known to facilitate the proteosomal degradation of IRS-1 leading to the down-regulation of insulin signalling at IRS-1 in 3T3-L1 adipocytes [17–19]. However, it is unknown whether SHIP2 is also involved in the resistance caused by chronic exposure to insulin. In the present study, the change in SHIP2 expression following chronic insulin treatment was investigated in 3T3-L1 adipocytes. In addition, the effect of inhibition of endogenous SHIP2 function using adenovirus-mediated gene transfer of a dominant-negative SHIP2 (ΔIP-SHIP2) on the possible amelioration of decreased insulin signalling caused by the chronic insulin treatment was investigated. The down-regulation of insulin signalling at the level of IRS-1 caused by the chronic insulin treatment can be ameliorated by pretreatment with rapamycin, which is an inhibitor of mTOR-dependent proteosomal degradation of IRS-1 [20, 21]. Alternatively, the decrease of IRS-1 can be prevented by overexpression of IRS-1 through adenovirus-mediated gene transfer [22]. Finally, the effects of the amelioration at the level of IRS-1 and SHIP2 on the chronic insulin treatment-induced down-regulation of insulin signalling were compared.

Materials and methods

Materials Human crystal insulin was provided by Novo Nordisk Pharmaceutical (Copenhagen, Denmark). [γ-^{32}P] ATP (111 TBq/mmol) and 2-[^{3}H]deoxyglucose (DOG; 3,330 GBq/mmol) were purchased from NEN Life Science Products (Boston, MA, USA). The two polyclonal anti-SHIP2 antibodies were described previously [7]. A polyclonal anti-PKCλ antibody was kindly provided by Dr W. Ogawa (Kobe University, Japan) [22]. A monoclonal anti-phosphotyrosine antibody (PY99) was from Transduction Laboratories (Lexington, KY, USA). A polyclonal anti-Thr^{308} phospho-specific Akt antibody, a polyclonal anti-Ser^{473} phospho-specific Akt antibody, and a monoclonal anti-PKCλ antibody were from Cell Signalling (Beverly, MA, USA). A polyclonal anti-Akt antibody and a polyclonal anti-Glut4 antibody were from Santa Cruz Biotechnology (Santa Cruz, CA, USA). A polyclonal IRS-1 antibody and a polyclonal anti-PDGF β receptor antibody were from Upstate Biotechnology (Lake Placid, NY, USA). Enhanced chemiluminescence reagents were from Amersham Pharmacia Biotech (Uppsala, Sweden). Dulbecco's modified Eagle's medium (DMEM), minimum essential medium (MEM) vitamin mixtures, and MEM amino acid solutions were from Gibco BRL Japan (Tokyo, Japan). All other reagents were of analytical grade and purchased from Sigma Chemical (St Louis, MO, USA) or Wako Pure Chemical Industries (Osaka, Japan).

Construction of adenoviral vectors A cDNA encoding a phosphatidylinositol 5′-phosphatase-defective mutant of SHIP2 (ΔIP-SHIP2) containing Pro^{687} to Ala, Asp^{691} to Ala, and Arg^{692} to Gly changes was subcloned into the vector pAxCAwt, and transferred to recombinant adenovirus by homologous recombination utilizing an Adenovirus Expression Vector Kit (Takara Biomedicals, Tokyo, Japan) as described previously [8]. The adenoviral vector encoding IRS-1 was also described previously [23].

Cell culture and infections with adenovirus 3T3-L1 fibroblasts were grown and passaged in DMEM supplemented with 10% donor calf serum. Cells at 2–3 days postconfluence were used for differentiation. The differentiation medium contained 10% fetal bovine serum (FBS), 250 nmol/l dexamethasone, 0.5 mmol/l isobutyl methylxanthine, and 500 nmol/l insulin. After 3 days, the differentiation medium was replaced with postdifferentiation medium containing 10% FBS and 500 nmol/l insulin. After 3 more days, the postdifferentiation medium was replaced with DMEM supplemented with 10% FBS. ΔIP-SHIP2 and IRS-1 were transiently expressed in differentiated 3T3-L1 adipocytes by means of adenovirus-mediated gene transfer. A multiplicity of infection (m.o.i.) of 10–40 pfu/cell was used to infect 3T3-L1 adipocytes in DMEM containing 2% FBS, with the virus being left on the cells for 16 h prior to removal. Subsequent experiments were conducted 24–48 h after initial addition of the virus [8]. The efficiency of adenovirus-mediated gene transfer of ΔIP-SHIP2 and IRS-1 was approximately 95%.

Measurements of PI(3,4,5)P3 and PI(3,4)P2 levels in vivo The same numbers of 3T3-L1 adipocytes transfected with LacZ or ΔIP-SHIP2 were starved of phosphate overnight in phosphate-free DMEM (Life Technology), then starved of serum for 3 h. [^{32}P]Orthophosphate (3.7 MBq/ml) was added, and the cells were cultured for an additional 2 h. Following the labelling period, the cells were incubated with or without 1 μmol/l insulin for 15 min. The reaction was terminated by washing once with ice-cold PBS, followed by the addition of methanol and 1 N HCl (1:1). The labelling of the cells with [^{32}P]orthophosphate was con-

ducted at the same time in both sets of transfected cells. Phospholipids were then extracted with chloroform. The extracted lipid was deacylated and subjected to amino-exchange high-performance liquid chromatography (HPLC) using a Partisphere strong anion-exchange column (Whatman) as described previously [8]. The PI(3,4)P2 and PI(3,4,5)P3 levels in the same sample for each line were measured within a single HPLC run. The radioactivity was detected with an online radiochemical detector.

Chronic insulin treatment 3T3-L1 adipocytes grown in 6-well multiplates were incubated with DMEM containing 0.1% FBS with or without 100 nmol/l insulin at 37°C for various periods. For experiments with rapamycin treatment, 20 nmol/l rapamycin was added for 30 min before the addition of insulin. At the end of the chronic treatment with insulin, the cells were washed with PBS, incubated in serum-free DMEM for 30 min, and washed again with PBS. The cells were then treated with or without 17 nmol/l insulin for 5 min.

Plasma membrane fractionation The cells were washed twice with PBS and once with HES buffer (255 mmol/l sucrose, 20 mmol/l HEPES, 1 mmol/l EDTA, 1 mmol/l phenylmethylsulphonyl fluoride [PMSF], 1 mmol/l Na_3VO_4, 2 μg/ml of aprotinin, and 50 ng/ml of okadaic acid, pH 7.4) and immediately homogenized by 20 strokes with a motor-driven homogenizer in HES buffer at 4°C. The homogenates (two 10-cm-diameter dishes per condition) were subjected to subcellular fractionation as described previously to isolate the plasma membrane (PM) [21]. In brief, the homogenates were centrifuged at 19,000 *g* for 20 min. The pellet obtained from the spin was resuspended in HES buffer, layered onto a 1.12 mol/l sucrose cushion, and centrifuged at 100,000 *g* in a swing rotor for 60 min. A white fluffy band at the interface was collected, resuspended in HES buffer, and centrifuged at 40,000 *g* for 20 min, yielding a pellet of PM. All fractions were adjusted to a final protein concentration of 1–3 mg/ml, which was measured by the Bradford method, and stored at −80°C until use.

Immunoprecipitation and western blotting The cells or the plasma membrane preparation were lysed in a buffer containing 20 mmol/l Tris, 150 mmol/l NaCl, 1 mmol/l EDTA, 1 mmol/l EGTA, 2.5 mmol/l sodium deoxycholate, 1 mmol/l β-glycerophosphate, 1% Triton X-100, 1 mmol/l PMSF, 1 mmol/l Na_3VO_4, 50 mmol/l sodium fluoride, 10 μg/ml of aprotinin, and 10 μmol/l leupeptin, pH 7.4, for 30 min at 4°C. The lysates were centrifuged to remove insoluble materials. The supernatants (100 μg of protein) were immunoprecipitated with antibodies for 2 h at 4°C. The precipitates or the lysates were then separated by 7.5% SDS-PAGE and transferred onto polyvinylidene difluoride membranes (PVDM) using a Bio-Rad Transblot apparatus. The membranes were blocked in a buffer containing 50 mmol/l Tris, 150 mmol/l NaCl, 0.1% Tween 20, and 2.5% bovine serum albumin (BSA) or 5% non-fat milk, pH 7.5, for 2 h at 20°C. They were then probed with antibodies for 2 h at 20°C or for 16 h at 4°C. After the membranes were washed in a buffer containing 50 mmol/l Tris, 150 mmol/l NaCl, and 0.1% Tween 20, pH 7.5, blots were incubated with a horseradish peroxidase-linked secondary antibody and subjected to enhanced chemiluminescence detection using ECL reagent according to the manufacturer's instructions (Amersham) [8]. In each experiment, the intensity of the band derived from control cells was assigned a value of 1 arbitrary unit, and the intensity of all treated groups was expressed as a fold value of control.

Measurement of PKCλ activity The cells were washed with ice-cold PBS and lysed with PKCλ buffer containing 50 mmol/l MOPS–HCl, 0.5% Triton X-100, 10% glycerol, 5 mmol/l EDTA, 5 mmol/l EGTA, 20 mmol/l NaF, 50 mmol/l β-glycerophosphate, 2 mmol/l Na_3VO_4, 2 mmol/l DTT, 1 μg/ml of leupeptin, and 2 mmol/l PMSF, pH 7.5. The lysates were centrifuged at 15,000 *g* for 20 min. The protein concentration in the resulting supernatants was determined with the use of bicinchoninic acid protein assay reagent (Pierce), and equal amounts of protein were subjected to immunoprecipitation with anti-PKCλ antibody. The immunoprecipitates were washed twice with PKCλ buffer containing 0.1% BSA, once with PKCλ buffer containing 0.1% BSA and 1 mol/l NaCl, and once with a solution containing 20 mmol/l Tris–HCl, 10% glycerol, 0.5 mmol/l EDTA, 0.5 mmol/l EGTA, 20 mmol/l 2-mercaptoethanol, 10 μg/ml of leupeptin, and 2 mmol/l PMSF, pH 7.5. Then, the precipitates were incubated for 14 min at 30°C with 14.8 kBq of [γ-^{32}ATP] in a reaction mixture (25 μl) containing 35 mmol/l Tris, pH 7.5, 10 mmol/l $MgCl_2$, 0.5 mmol/l EGTA, 0.1 mmol/l $CaCl_2$, 40 μmol/l unlabelled ATP, 100 μg/ml of phosphatidylserine, and 30 μmol/l myelin basic protein (MBP) as a substrate. Kinase reactions were terminated by the addition of SDS sample buffer, and the samples were then fractionated by SDS-PAGE [8, 22]. The radioactivity incorporated into substrates was determined with a Fuji BAS 2000 image analyser.

Measurement of 2-DOG uptake 3T3-L1 adipocytes grown in 6-well multiplates were serum-starved for 3 h. The cells were treated with or without rapamycin for 30 min and further incubated with 17 nmol/l insulin for 6 h. The cells were washed once with PBS, three times with Krebs–Ringer phosphate (KRP)–HEPES buffer, 10 nmol/l HEPES, 131.2 mmol/l NaCl, 4.7 mmol/l KCl, 1.2 mmol/l $MgSO_4$, 2.5 mmol/l $CaCl_2$, and 2.5 mmol/l NaH_2PO_4, pH 6.0, and once with KRP–HEPES buffer containing 1% BSA, pH 7.4. The cells were then incubated with the same KRP–HEPES buffer for 1 h at 37°C. The cells were subsequently stimulated with various concentrations of insulin. Following 15 min of insulin treatment, 3.7 kBq of 2-[^{3}H] DOG was added for 4 min. The reaction was stopped by the addition of 10 μmol/l cytochalasin B. The cells were washed three times with PBS and solubilized with 0.2 mmol/l SDS–0.2 N NaOH [8]. The radioactivity incorporated into the cells was measured by liquid scintillation counting.

Statistical analysis The data are represented as means ± SEM. p Values were determined using Student's t test, and $p<0.05$ was considered statistically significant.

Results

Effect of chronic insulin treatment on IRS-1 and SHIP2 Chronic treatment with insulin facilitates the proteosomal degradation of IRS-1 [20, 21, 24, 25]. Treatment with insulin reduced the amount of IRS-1, but not Akt, in a time-dependent manner in 3T3-L1 adipocytes. After 12 h of treatment, the amount of IRS-1 was 13.6±2.6% of the control level (Fig. 1a). In accordance with the reduced amount of IRS-1, the subsequent insulin-stimulated tyrosine phosphorylation of IRS-1 following chronic insulin treatment was markedly decreased to 13.2±1.8% (Fig. 1b). Thus, chronic insulin treatment caused an impairment of insulin signalling, at least, at the step involving IRS-1. Since SHIP2 is an important negative regulator of insulin signalling, alteration of its expression may cause insulin resistance [8–12]. In this regard, the amount of SHIP2 protein was relatively high after chronic treatment with insulin. Following 6 h of insulin treatment, the amount of SHIP2, but not Akt, was increased by 36.4±7.4% (Fig. 1c). Membrane targeting of SHIP2 is known to be important to its function to hydrolyse PI(3,4,5)P3 in insulin signalling [26]. The extent of insulin-induced translocation of SHIP2 to the plasma membrane fraction was increased by 33.4±8.3% compared to that without chronic insulin treatment. To assure equal amounts of protein were loaded among the samples, the PM fraction was immunoblotted with anti-PDGF β receptor antibody (Fig. 1d). These results indicate that chronic insulin treatment elicits insulin resistance, at least in part, at the level of SHIP2 as well as IRS-1.

Inhibition of endogenous SHIP2 function by expression of ΔIP-SHIP2 Because an elevated amount of SHIP2, especially at the plasma membrane, appears to be involved in the insulin resistance caused by the chronic insulin treat-

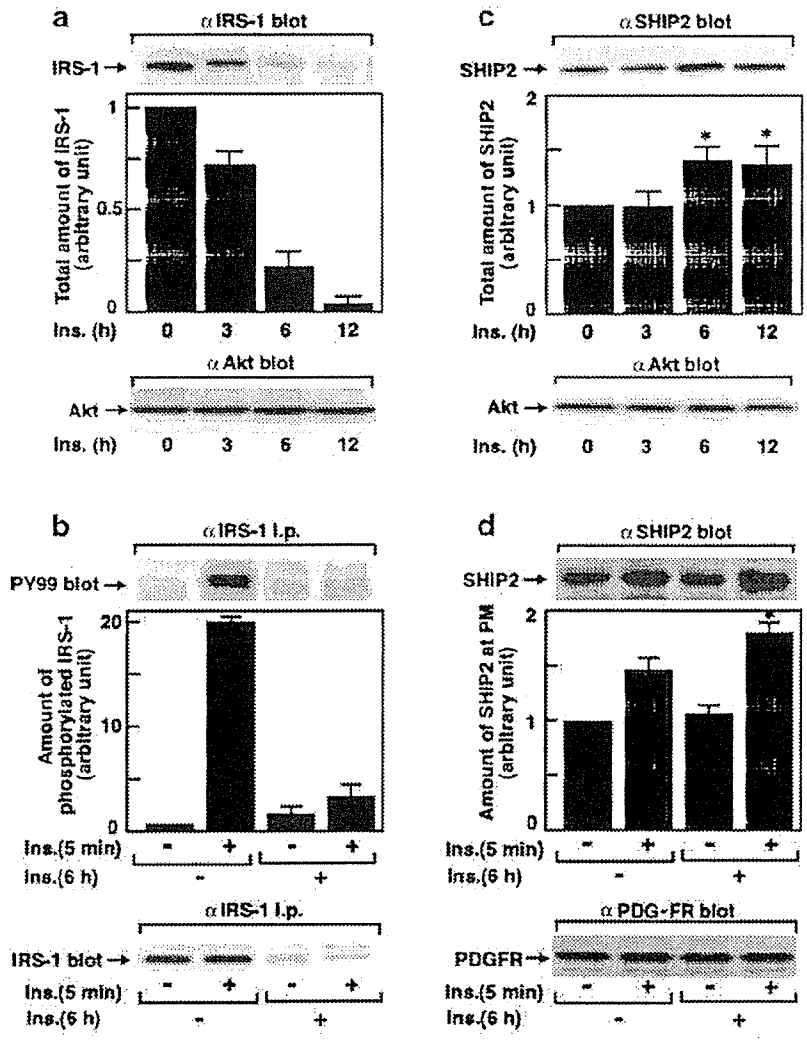

Fig. 1 Effect of chronic insulin treatment on IRS-1 and SHIP2. 3T3-L1 adipocytes were treated with 17 nmol/l insulin for the periods indicated (chronic insulin treatment). **a** The cells were lysed, and the proteins were separated by SDS-PAGE and immunoblotted with anti-IRS-1 antibody or anti-Akt antibody. **b** After chronic insulin treatment, the cells were washed with PBS and incubated in insulin-free medium for 30 min, then stimulated with 17 nmol/l insulin for 5 min (acute insulin treatment). The cell lysates were immunoprecipitated with anti-IRS-1 antibody. The precipitates were subjected to SDS-PAGE, and immunoblotted with anti-phosphotyrosine antibody (PY99) or anti-IRS-1 antibody. **c** The cell lysates were separated by SDS-PAGE and immunoblotted with anti-SHIP2 antibody or anti-Akt antibody. *$p<0.05$ versus amounts of SHIP2 without chronic insulin treatment. **d** The cells were homogenized and subjected to subcellular fractionation to yield the plasma membrane (PM) fraction. Samples in the PM fraction were separated by SDS-PAGE and immunoblotted with anti-SHIP2 antibody or anti-PDGF β receptor antibody. *$p<0.05$ versus amounts of SHIP2 at PM following 5 min of insulin stimulation without chronic insulin treatment. Results are means ± SEM of three separate experiments.

ment, expression of ΔIP-SHIP2, which acts in a dominant-negative manner, may ameliorate the impaired insulin signalling. Adenovirus-mediated gene transfer produced an eightfold increase in ΔIP-SHIP2 expression compared to the endogenous level of SHIP2 (Fig. 3b). The expression of ΔIP-SHIP2 increased insulin-induced generation of PI(3,4,5)P3, whereas the amount of PI(3,4)P2 was decreased (Fig. 2a). Thus, the expression of ΔIP-SHIP2 in fact functions to inhibit the endogenous 5′-phosphatase activity of SHIP2 in 3T3-L1 adipocytes. In addition, insulin-induced increase in the levels of PI(3,4,5)P3 was decreased to 25% after chronic insulin exposure. ΔIP-SHIP2 expression ameliorated the reduced levels of PI (3,4,5)P3 to 61% of the control level (data not shown). Thus, expression of ΔIP-SHIP2 appears to effectively ameliorate the decreased PI(3,4,5)P3 levels caused by chronic insulin treatment.

Effect of ΔIP-SHIP2 and IRS-1 expression, and pretreatment with rapamycin on insulin-induced phosphorylation of Akt after chronic insulin treatment Treatment with PI3-kinase inhibitor LY294002 effectively inhibited the chronic insulin treatment-induced degradation of IRS-1. Expression of ΔIP-SHIP2 partly abolished the inhibitory effect of LY294002 on the IRS-1 degradation, because SHIP2 is located downstream of PI3-kinase (data not shown). These results indicate that chronic insulin treatment induces the degradation of IRS-1 via PI3-kinase dependent mechanism. mTOR is a downstream molecule of PI3-kinase, and rapamycin is known to efficiently inhibit mTOR-dependent proteosomal degradation of IRS-1 in 3T3-L1 adipocytes [19–21]. Thus, the decrease in the amount of IRS-1 induced by degradation after chronic insulin treatment was effectively prevented by pretreatment with rapamycin. In contrast, expression of ΔIP-SHIP2 alone did not affect the loss of IRS-1 caused by the chronic insulin treatment. In addition, the preventive effect of rapamycin was not affected by the expression of ΔIP-SHIP2, because SHIP2 is located upstream of mTOR [8]. The decrease in IRS-1 caused by chronic insulin treatment can also be prevented by advanced overexpression of IRS-1. Thus, overexpression of IRS-1 in advance prevented the decrease in IRS-1 caused by chronic insulin treatment in an m.o.i.-dependent manner (data not shown). At an m.o.i. of 10 pfu/cell, the amount of IRS-1 after chronic insulin treatment was similar to that without chronic insulin treatment. The amount of protein loaded among the samples was confirmed to be identical by immunoblotting with anti-Akt antibody (Fig. 3b). As a result, rapamycin treatment and IRS-1 overexpression ameliorated the decreased levels of PI(3,4,5)P3 by chronic insulin treatment to 52% and 58%, respectively, of the control level (data not shown). Akt is an important mediator of the metabolic actions of insulin, and the activation of Akt is induced by the phosphorylation at Thr^{308} and Ser^{473} [8, 26–28]. Chronic insulin treatment decreased the subsequent insulin-stimulated phosphorylation of Akt at Thr^{308} and Ser^{473} to 23.8 ±2.0% and 28.5±2.1%, respectively. The reduction can be caused by the alteration of IRS-1 and/or SHIP2 following chronic insulin treatment. In this regard, pretreatment with rapamycin ameliorated the insulin-induced phosphorylation of Akt at Thr^{308} and Ser^{473}. Similarly, overexpression of ΔIP-SHIP2 effectively ameliorated the phosphorylation of Akt at Thr^{308} and Ser^{473} in an m.o.i.-dependent manner (data not shown), and it was most effectively ameliorated at an m.o.i. of 40 pfu/cell. The amelioration was more apparent and almost fully restored to the control level by both pretreatment with rapamycin and expression of ΔIP-SHIP2. In addition, the effective restoration of insulin-stimulated phosphorylation of Akt following chronic insulin treatment was also seen after advanced overexpression of IRS-1 (Fig. 3a).

Effect of ΔIP-SHIP2 and IRS-1 expression, and pretreatment with rapamycin, on insulin-induced activation of PKCλ after chronic insulin treatment Another important molecule downstream of PI3-kinase for metabolic insulin signalling is atypical PKC in 3T3-L1 adipocytes [22, 29]. In accordance with the results of insulin-induced phosphorylation of Akt, insulin stimulation of PKCλ activity was decreased to 23.8±3.9% of the control level after chronic insulin treatment. Pretreatment with rapamycin

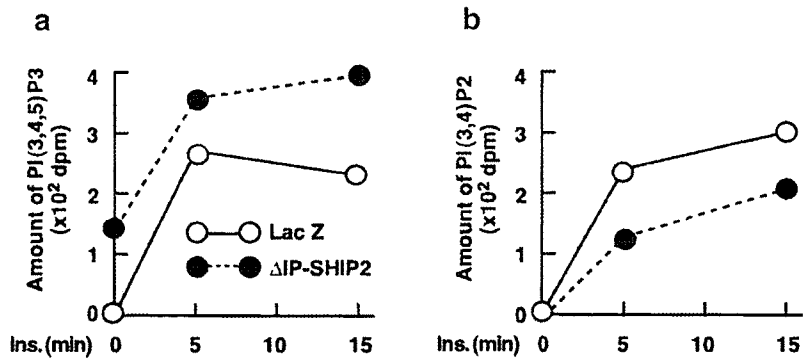

Fig. 2 Inhibition of endogenous SHIP2 function by expression of ΔIP-SHIP2. 3T3-L1 adipocytes were transfected with LacZ or ΔIP-SHIP2 at an m.o.i. of 40 pfu/cell. The cells were labelled with [^{32}P] orthophosphate for 2 h and incubated with or without insulin, and lipids were extracted with chloroform. The extracted lipids were analysed by HPLC after being deacylated. The amounts of ^{32}P-labelled PI(3,4,5)P3 (**a**) and PI(3,4)P2 (**b**) generated were determined with an online radiochemical detector. Results are means of two separate experiments.

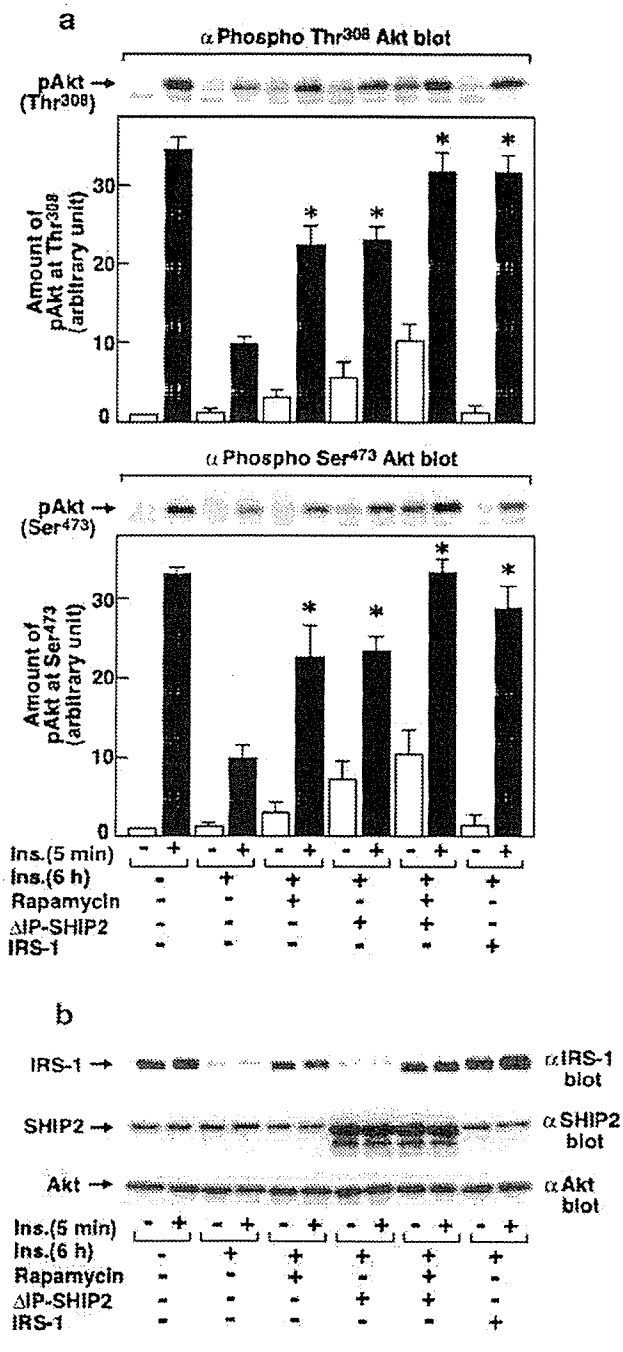

◀ **Fig. 3** Effect of ΔIP-SHIP2 and IRS-1 expression, and pretreatment with rapamycin on insulin-induced phosphorylation of Akt after chronic insulin treatment. 3T3-L1 adipocytes were transfected with LacZ and ΔIP-SHIP2 at an m.o.i of 40 pfu/cell, or IRS-1 at an m.o.i. of 10 pfu/cell. Serum-starved transfected cells were incubated with vehicle or 20 nmol/l rapamycin for 30 min, and treated with 17 nmol/l insulin for 6 h. The cells were washed with PBS and incubated in insulin-free medium for 30 min, and the cells were stimulated with 17 nmol/l insulin for 5 min. **a** The cells were lysed and the lysates were separated by SDS-PAGE and immunoblotted with anti-Ser^{473}-phospho-specific or anti-Thr^{308}-phospho-specific Akt antibody. The amount of Akt phosphorylated at Ser^{473} and Thr^{308} was quantitated by densitometry. Results are means ± SEM of four separate experiments. $^*p<0.05$ versus amounts of phosphorylated Akt in LacZ-transfected cells with chronic insulin treatment. **b** The cell lysates were separated by SDS-PAGE, and immunoblotted with anti-IRS-1 antibody, anti-SHIP2 antibody, or anti-Akt antibody.

only partly restored the decreased PKCλ activity to 49.8± 3.8%. Although the effect was still partial, expression of ΔIP-SHIP2 relatively efficiently ameliorated the reduced PKCλ activity caused by the chronic insulin treatment to 65.0±7.5% of the control level. A combination of rapamycin treatment and expression of ΔIP-SHIP2 more effectively restored the insulin-induced activation of PKCλ. In contrast to the results for the phosphorylation of Akt, the restoration of PKCλ activity was still partial, and was 75.2±4.1% of the control level. The partial amelioration of insulin-stimulated PKCλ activity after chronic insulin treatment was also seen with advanced overexpression of IRS-1 (Fig. 4a). The amount of PKCλ protein was not

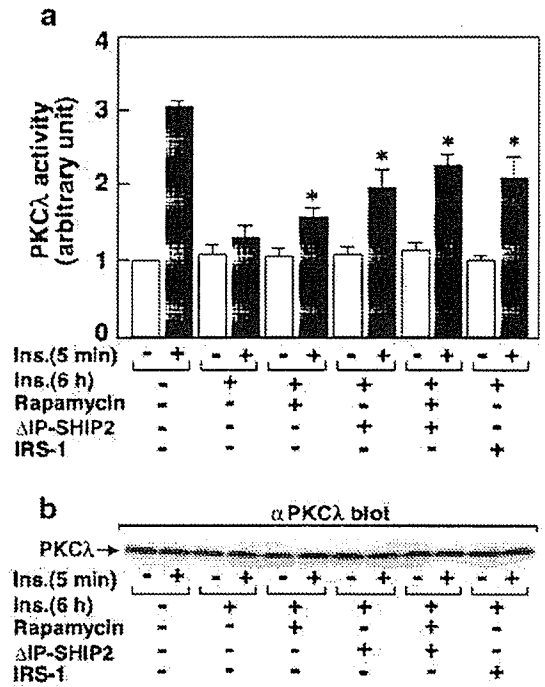

Fig. 4 Effect of ΔIP-SHIP2 and IRS-1 expression, and pretreatment with rapamycin, on insulin-induced activation of PKCλ after chronic insulin treatment. 3T3-L1 adipocytes were transfected with LacZ and ΔIP-SHIP2 at an m.o.i. of 40 pfu/cell, or IRS-1 at an m.o.i. of 10 pfu/cell. Serum-starved transfected cells were incubated with vehicle or 20 nmol/l rapamycin for 30 min, and treated with 17 nmol/l insulin for 6 h. The cells were washed with PBS, incubated in insulin-free medium for 30 min, and stimulated with 100 nmol/l insulin for 5 min. They were then lysed and immunoprecipitated with anti PKCλ antibody. Kinase reactions were conducted, and samples were fractionated by SDS-PAGE. **a** The radioactivity incorporated into substrates was determined with a Fuji BAS 2000 image analyser. Results are means ± SEM of three separate experiments; $^*p<0.05$ versus insulin-stimulated PKCλ activity in LacZ-transfected control cells with chronic insulin treatment. **b** The cell lysates were separated by SDS-PAGE, and immunoblotted with anti-PKCλ antibody.

altered either by chronic insulin treatment, treatment with rapamycin, or expression of ΔIP-SHIP2 and IRS-1 (Fig. 4b).

Effect of ΔIP-SHIP2 and IRS-1 expression, and pretreatment with rapamycin, on insulin-induced 2-DOG uptake after chronic insulin treatment Since insulin-stimulated phosphorylation of Akt and PKCλ activity decreased by the chronic insulin treatment was ameliorated by rapamycin treatment and expression of ΔIP-SHIP2 and IRS-1, we next examined these effects on insulin stimulation of 2-DOG uptake (Fig. 5a). Again, insulin-induced 2-DOG uptake was markedly decreased to 25.6±5.2% after chronic insulin treatment. Pretreatment with rapamycin and expression of ΔIP-SHIP2 partially restored the decreased 2-DOG uptake to 47.5±3.7% and 54.4±4.1%, respectively, of the control level. Both rapamycin treatment and ΔIP-SHIP2 expression more efficiently ameliorated the reduced 2-DOG uptake to 69.2±4.4%. Advanced overexpression of IRS-1 also improved the reduced 2-DOG uptake to 69.7 ±2.5% of the control level. The amount of Glut4 protein was not altered either by chronic insulin treatment, treatment with rapamycin, or overexpression of ΔIP-SHIP2 and IRS-1 (Fig. 5b).

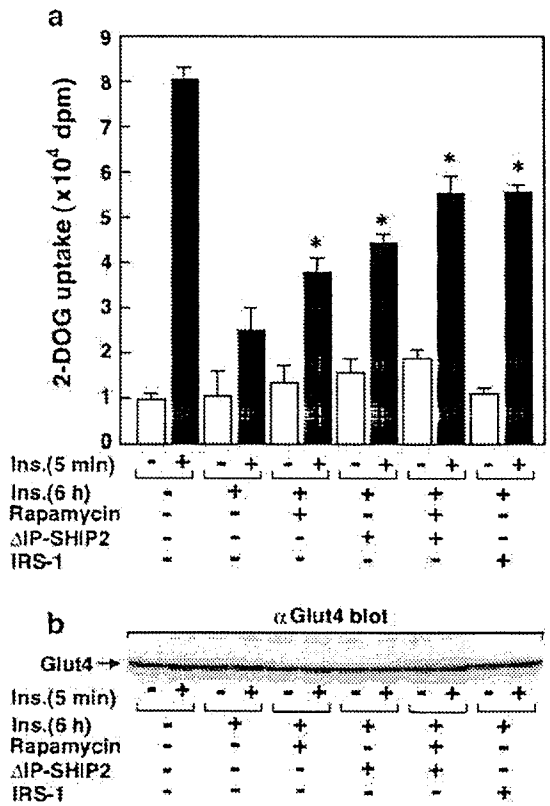

Fig. 5 Effect of ΔIP-SHIP2 and IRS-1 expression, and pretreatment with rapamycin, on insulin-induced 2-DOG uptake after chronic insulin treatment. 3T3-L1 adipocytes were transfected with LacZ and ΔIP-SHIP2 at an m.o.i. of 40 pfu/cell, or IRS-1 at an m.o.i. of 10 pfu/cell. Serum-starved transfected cells were incubated with vehicle or 20 nmol/l rapamycin for 30 min, and treated with 100 nmol/l insulin for 6 h. The cells were washed with PBS, incubated in insulin-free medium for 3 h, and washed again with PBS and incubated in glucose-free medium for another 30 min. After the cells had been stimulated with 10 nmol/l insulin for 5 min, 3.7 kBq of 2-[^{3}H]DOG was added for 3 min. The reaction was stopped by the addition of 10 μmol/l cytochalasin B. The cells were washed three times with PBS and solubilized with 0.2 mmol/l SDS–0.2 N NaOH. **a** The radioactivity incorporated into the cells was measured with a liquid scintillation counter. Results are means ± SEM of three separate experiments. *$p<0.05$ versus insulin-induced 2-DOG uptake in LacZ-transfected control cells with chronic insulin treatment. **b** The cell lysates were separated by SDS-PAGE and immunoblotted with anti-Glut4 antibody.

Discussion

Chronic insulin exposure is known to cause a subsequent insulin resistance, by reducing the level of IRS-1 via PI3-kinase and rapamycin-dependent pathways [17–21, 30, 31]. In fact, our results demonstrated that chronic insulin treatment induced a reduction in IRS-1 levels in a time-dependent manner. In addition to the impaired IRS-1–dependent signalling pathway, the present study showed increased amounts of SHIP2 following chronic insulin exposure. Since SHIP2 is the physiologically important negative regulator of insulin signalling with a fundamental impact on the state of insulin resistance [8–12], the increase in SHIP2 protein appears to be part of the novel molecular mechanism of insulin resistance caused by chronic insulin treatment. Because SHIP2 is translocated to the plasma membrane where it functions to hydrolyse PI(3,4,5)P3, the increase in the amount of SHIP2 protein in the plasma membrane preparation further supports the possible involvement of SHIP2 in insulin resistance in 3T3-L1 adipocytes [26].

We employed two approaches to ameliorate the decrease in IRS-1 levels caused by the chronic insulin treatment. As shown in Fig. 3, pretreatment with rapamycin prevented the mTOR-dependent proteosomal degradation of IRS-1 caused by the chronic insulin treatment. Overexpression of exogenous IRS-1 in advance normalized the decreased IRS-1 levels caused by the insulin treatment. On the other hand, endogenous SHIP2 function was efficiently inhibited by expression of the 5′-phosphatase defective dominant-negative SHIP2 (ΔIP-SHIP2) as shown in Fig. 2. These approaches would be useful for clarifying whether the rescue of insulin signalling at the level of IRS-1 and/or SHIP2 is effective in ameliorating insulin resistance caused by chronic insulin treatment. The decrease in the phosphorylation of Akt caused by the chronic insulin treatment was effectively ameliorated by either prevention of the decrease in IRS-1 by rapamycin treatment or advanced IRS-1 overexpression, or inhibition of endogenous SHIP2 function by expression of the dominant-negative SHIP2 (ΔIP-SHIP2). These results indicate that insulin-induced phosphorylation of Akt is closely associated with the IRS-1–mediated PI3-kinase pathway. In addition, the full input of insulin signal does not appear to be required for the sufficient phosphorylation of Akt, because amelioration of insulin signalling at the step involving IRS-1

or SHIP2 is sufficient for the efficient restoration of the phosphorylation of Akt.

Phosphorylation at both Thr^{308} and Ser^{473} is required for the full activation of Akt [8, 26–28]. In this context, our results showed that the rescue of IRS-1 levels by treatment with rapamycin and overexpression of IRS-1 in advance, and expression of the dominant-negative SHIP2 (ΔIP-SHIP2), efficiently ameliorated the decreased insulin-induced phosphorylation of Akt at both residues caused by the chronic insulin treatment. In contrast to the effective recovery of acute insulin stimulation of Akt phosphorylation, the recovery of acute insulin stimulation of PKCλ activation was only partial for both the restoration of IRS-1 levels and inhibition of SHIP2 function. Thus, pretreatment with rapamycin, advanced IRS-1 overexpression, and ΔIP-SHIP2 expression only partially ameliorated the insulin-induced activation of PKCλ to 49.8±3.8%, 67.2± 8.5%, and 65.0±7.5%, respectively, of the control value. The rescue of the PKCλ activity was still partial with a combination of ΔIP-SHIP2 expression and rapamycin pretreatment (or IRS-1 expression—data not shown). Therefore, the insulin resistance caused by chronic treatment may also impair insulin signalling at the step important for PKCλ activation more directly in addition to the IRS-1–PI3-kinase pathway. It is possible that another insulin signalling system important for glucose uptake including the CAP–Cbl–TC10 pathway may be a candidate implicated in the signalling step, although further investigation is needed to clarify the issue [32, 33]. We can not rule out the possibility that full activation of the IRS-1–PI3-kinase pathway is required for the efficient activation of PKCλ, although resistance at the levels of IRS-1 and SHIP2 appears to be efficiently rescued by pretreatment with rapamycin and expression of ΔIP-SHIP2.

Interestingly, the decreased stimulation of 2-DOG uptake caused by chronic insulin treatment was only partly restored by the maintenance of IRS-1 levels by pretreatment with rapamycin or advanced overexpression of IRS-1, or expression of ΔIP-SHIP2 as shown in Fig. 5. These findings are consistent with the results of PKCλ activation, and not Akt activation. Although Akt and atypical PKC are downstream effectors of PI3-kinase strongly implicated in the metabolic actions of insulin, the relative importance of Akt versus atypical PKC in insulin-induced 2-DOG uptake is controversial [8, 22, 27–29, 34]. Our results indicate that PKCλ/ζ rather than Akt may be more closely linked to the insulin-stimulated glucose uptake and associated with the state of insulin resistance. It is unclear whether this difference between Akt and PKCλ activation in chronic insulin treatment reflects a small input of IRS-1–dependent insulin signalling sufficient for Akt activation, or whether factors other than IRS-1–dependent insulin signalling are involved in the impairment of PKCλ activation. In any event, our results indicate that PKCλ activity rather than Akt activity appears to be associated with the decreased glucose uptake caused by chronic insulin treatment. Regardless of the importance of PKCλ to the state of insulin resistance, overexpression of the constitutively active form of PKCλ did not completely rescue the decreased insulin-stimulated glucose uptake caused by the chronic insulin treatment (data not shown). Based on this observation, chronic insulin treatment appears to cause insulin resistance at multiple signalling steps including a step distal to the PKCλ activation leading to the glucose uptake. It is also possible that chronic insulin treatment impairs the glucose uptake involved in the Glut4 translocation system independent of insulin signalling as previously reported for the insulin resistance caused by dexamethasone treatment in 3T3-L1 adipocytes [23].

In summary, SHIP2 appears to participate in insulin resistance, at least in part, caused by chronic insulin treatment in 3T3-L1 adipocytes. In addition, (1) impaired early insulin signalling occurring mainly at IRS-1 for the PI3-kinase activation, (2) impaired insulin signalling for PKCλ activation, and (3) impaired glucose transport system may also be involved in the insulin resistance caused by chronic insulin treatment. Furthermore, the present study indicates that the inhibition of endogenous SHIP2 appears to be effective at ameliorating the insulin signal in a state of insulin resistance, and that the activity of PKCλ rather than Akt may be more closely associated with the decreased 2-DOG uptake caused by the chronic insulin treatment in 3T3-L1 adipocytes. Taken together, inhibition of the endogenous level and/or function of SHIP2 would be an important therapeutic target of insulin resistance in type 2 diabetes.

Acknowledgements This work was supported in part by a grant-in-aid for scientific research from the Japan Society for the Promotion of Science. We thank Dr Wataru Ogawa (Kobe University, Japan) for kindly providing the anti-PKCλ antibody and Dr Kazuyuki Hiratani (Toyama Medical and Pharmaceutical University, Japan) for technical assistance. T. Sasaoka and K. Fukui contributed equally to this work.

References

1. Rameh LE, Cantley LC (1999) The role of phosphoinositide 3-kinase lipid products in cell function. J Biol Chem 274:8347–8350
2. Cantley LC (2002) The phosphoinositide 3-kinase pathway. Science 296:1655–1657
3. Virkamäki A, Ueki K, Kahn CR (1999) Protein–protein interaction in insulin signaling and the molecular mechanisms of insulin resistance. J Clin Invest 103:931–943
4. Czech MP, Corvera S (1999) Signaling mechanisms that regulate glucose transport. J Biol Chem 274:1865–1868
5. Saltiel AR, Pessin JE (2002) Insulin signaling pathways in time and space. Trends Cell Biol 12:65–71
6. Pesesse X, Deleu S, De Smedt F, Drayer L, Erneux C (1997) Identification of a second SH2-domain-containing protein closely related to the phosphatidylinositol polyphosphate 5-phosphatase SHIP. Biochem Biophys Res Commun 239:697–700
7. Ishihara H, Sasaoka T, Hori H et al (1999) Molecular cloning of rat SH2-containing inositol phosphatase 2 (SHIP2) and its role in the regulation of insulin signaling. Biochem Biophys Res Commun 260:265–272
8. Wada T, Sasaoka T, Funaki M et al (2001) Overexpression of SH2-containing inositol phosphatase 2 results in negative regulation of insulin-induced metabolic actions in 3T3-L1 adipocytes via its 5′-phosphatase catalytic activity. Mol Cell Biol 21:1633–1646

9. Sasaoka T, Hori H, Wada T et al (2001) SH2-containing inositol phosphatase 2 negatively regulates insulin-induced glycogen synthesis in L6 myotubes. Diabetologia 44:1258–1267
10. Clement S, Krause U, Desmedt F et al (2001) The lipid phosphatase SHIP2 controls insulin sensitivity. Nature 409:92–97
11. Hori H, Sasaoka T, Ishihara H et al (2002) Association of SH2-containing inositol phosphatase 2 with the insulin resistance of diabetic db/db mice. Diabetes 51:2387–2394
12. Marion E, Kaisaki PJ, Pouillon V et al (2002) The gene INPPL1, encoding the lipid phosphatase SHIP2, is a candidate for type 2 diabetes in rat and man. Diabetes 51:2012–2017
13. Reaven GM (1988) Role of insulin resistance in human disease. Diabetes 37:1595–1607
14. DeFronzo RA, Ferrannini E (1991) Insulin resistance: a multifaceted syndrome responsible for NIDDM, obesity, hypertension, dyslipidemia, and atherosclerotic cardiovascular disease. Diabetes Care 14:173–194
15. Goalstone ML, Natarajan R, Standley PR et al (1998) Insulin potentiates platelet-derived growth factor action in vascular smooth muscle cells. Endocrinology 139:4067–4072
16. Rondinone CM, Wang L-M, Lonnroth P, Wesslau C, Pierce JH, Smith U (1997) Insulin receptor substrate (IRS) 1 is reduced and IRS-2 is the main docking protein for phosphatidylinositol 3-kinase in adipocytes from subjects with non-insulin-dependent diabetes mellitus. Proc Natl Acad Sci U S A 94:4171–4175
17. Ricort J-M, Tanti J-F, Van Obberghen E, Le Marchand-Brustel Y (1995) Alterations in insulin signalling pathway induced by prolonged insulin treatment of 3T3-L1 adipocytes. Diabetologia 38:1148–1156
18. Thomson MJ, Williams MG, Frost SC (1997) Development of insulin resistance in 3T3-L1 adipocytes. J Biol Chem 272: 7759–7764
19. Berg CE, Lavan BE, Rondinone CM (2002) Rapamycin partially prevents insulin resistance induced by chronic insulin treatment. Biochem Biophys Res Commun 293:1021–1027
20. Haruta T, Uno T, Kawahara J et al (2000) A rapamycin-sensitive pathway down-regulates insulin signaling via phosphorylation and proteasomal degradation of insulin receptor substrate-1. Mol Endocrinol 14:783–794
21. Takano A, Usui I, Haruta T et al (2001) Mammalian target of rapamycin pathway regulates insulin signaling via subcellular redistribution of insulin receptor substrate 1 and integrates nutritional signals and metabolic signals of insulin. Mol Cell Biol 21:5050–5062
22. Kotani K, Ogawa W, Matsumoto M et al (1998) Requirement of atypical protein kinase Cλ for insulin stimulation of glucose uptake but not for Akt activation in 3T3-L1 adipocytes. Mol Cell Biol 18:6971–6982
23. Sakoda H, Ogihara T, Anai M et al (2000) Dexamethazone-induced insulin resistance in 3T3-L1 adipocytes is due to inhibition of glucose transport rather than insulin signal transduction. Diabetes 49:1700–1708
24. Sun XJ, Goldberg JL, Qiao L, Mitchell JJ (2002) Insulin-induced insulin receptor substrate-1 degradation is mediated by the proteasome degradation pathway. Diabetes 48:1359–1364
25. Zhande R, Mitchell JJ, Wu J, Sun XJ (2002) Molecular mechanism of insulin-induced degradation of insulin receptor substrate 1. Mol Cell Biol 22:1016–1026
26. Ishihara H, Sasaoka T, Ishiki M et al (2002) Membrane localization of src homology 2-containing inositol 5′-phosphatase 2 via Shc association is required for the negative regulation of insulin signaling in rat1 fibroblasts overexpressing insulin receptors. Mol Endocrinol 16:2371–2381
27. Kitamura T, Ogawa W, Sakaue H et al (1998) Requirement for activation of the serine-threonine kinase Akt (protein kinase B) in insulin stimulation of protein synthesis but not of glucose transport. Mol Cell Biol 18:3708–3717
28. Wang Q, Somwar R, Bilan PJ et al (1999) Protein kinase B/Akt participates in Glut4 translocation by insulin in L6 myoblasts. Mol Cell Biol 19:4008–4018
29. Bandyopadhyay G, Standaert ML, Zhao L et al (1997) Activation of protein kinase C (α, β, and ζ) by insulin in 3T3/L1 cells: transfection studies suggest a role for PKC-ζ in glucose transport. J Biol Chem 272:2551–2558
30. Pessin JE, Saltiel AR (2000) Signaling pathways in insulin action: molecular targets of insulin resistance. J Clin Invest 106:165–169
31. Sykiotis GP, Papavassiliou AG (2001) Serine phosphorylation of insulin receptor substrate-1: a novel target for the reversal of insulin resistance. Mol Endocrinol 15:1864–1869
32. Baumann CA, Ribon V, Kanzaki M et al (2000) CAP defines a second signalling pathway required for insulin-stimulated glucose transport. Nature 407:202–207
33. Chiang S-H, Baumann CA, Kanzaki M et al (2001) Insulin-stimulated Glut4 translocation requires the CAP-dependent activation of TC10. Nature 410:944–948
34. Bandyopadhyay G, Kanoh Y, Sajan MP, Standaert ML, Farese RV (2000) Effects of adenoviral gene transfer of wild-type, constitutively active, and kinase-defective protein kinase C-λ on insulin-stimulated glucose transport in L6 myotubes. Endocrinology 141:4120–4127

nature cell biology

Stat3-induced apoptosis requires a molecular switch in PI(3)K subunit composition

Kathrine Abell[1], Antonio Bilancio[2], Richard W. E. Clarkson[1], Paul G. Tiffen[1], Anton I. Altaparmakov[1], Thomas G. Burdon[3], Tomoichiro Asano[4], Bart Vanhaesebroeck[2,5] and Christine J. Watson[1,6]

Physiological apoptosis is induced by a switch from survival to death signalling. Dysregulation of this process is frequently associated with cancer[1]. A powerful model for this apoptotic switch is mammary gland involution, during which redundant milk-producing epithelial cells undergo apoptosis[2]. Signal transducer and activator of transcription 3 (Stat3) is an essential mediator of this switch but the mechanism has not yet been defined[3]. Stat3-dependent cell death during involution can be blocked by activation of Akt/protein kinase B (PKB)[4], a downstream effector of the phosphoinositide-3-OH kinase (PI(3)K) pathway[5]. Here we show that expression of the PI(3)K regulatory subunits p55α and p50α is induced by Stat3 during involution. In the absence of Stat3 *in vivo*, upregulation of p55α and p50α is abrogated, levels of activated Akt are sustained and apoptosis is prevented. Chromatin immunoprecipitation assays show that Stat3 binds directly to the p55α and p50α promoters *in vivo*. Overexpression of either p55α or p50α reduces levels of activated Akt. We propose a novel mechanism in which Stat3 regulates apoptosis by inducing expression of distinct PI(3)K regulatory subunits to downregulate PI(3)K-Akt-mediated survival signalling.

Stats are a family of latent transcription factors that mediate signalling from cytokines and growth factors[6]. Using conditional gene targeting, we have previously shown that activation of Stat3 is essential for the early phase of mammary gland involution because deletion of Stat3 resulted in reduced levels of apoptosis and delayed post-lactational regression[3]. Recently we found leukaemia inhibitory factor (LIF) to be the physiological activator of Stat3 *in vivo*[7], but so far the downstream effectors of this Stat3-dependent apoptotic signal have not been defined. Identification of these downstream effectors is important because constitutive Stat activity is often associated with tumorigenesis[8].

Involution is characterized by extensive apoptosis of the epithelial cells and a dramatic switch from survival to death signalling[2]. This apoptotic switch is exemplified in Fig. 1 showing that in involution the activity of the anti-apoptotic kinase Akt/PKB, as measured by its phosphorylation on Ser473, is downregulated (Fig. 1a, b) whereas Stat3 is activated (Fig. 1b). This change correlates with the induction of cell death as measured by a TdT-mediated dUTP nick end labelling (TUNEL) assay (Fig. 1a) and cleaved caspase-3 immunoblotting (Fig. 1b). Akt/PKB is activated in a PI(3)K-dependent manner[5] and negatively regulated by the tumour suppressor PTEN[9]. Transgenic expression of constitutively active mutants of Akt/PKB inhibit the induction of mammary epithelial cell death[4], thus overriding the pro-apoptotic signal from Stat3. It is therefore important for Akt/PKB to be downregulated in order to shift the balance in favour of the pro-apoptotic effects of Stat3.

To determine the mechanism by which Akt/PKB is downregulated at the apoptotic switch, we examined the expression level of PTEN, by western blot analysis (Fig. 1b). Surprisingly, the protein level of PTEN is also substantially reduced in involution, indicating that PTEN is unlikely to be the mechanism of phospho-Akt/PKB (pAkt/PKB) downregulation. We therefore measured the activity of PI(3)K across the lactation–involution transition (Fig. 1c) and found that pan-p85-associated PI(3)K activity was reduced threefold in involution compared with lactation. This provides an explanation for the low levels of pAkt/PKB in involution.

The reciprocal activation of Stat3 and Akt/PKB at the apoptotic switch prompted us to investigate whether there is any cross-talk between these death and survival pathways, by using tissue from mammary glands that are deficient in Stat3. Figure 1d shows that the level of pAkt/PKB and Akt/PKB is high in lactating control mice and that both forms are downregulated at the onset of involution. In contrast, pAkt/PKB activity was sustained in involuting Stat3-deficient mammary glands whereas total levels of Akt/PKB were diminished. We can conclude that Stat3 is a negative regulator of pAkt/PKB, but not total Akt/PKB, and that the levels of pAkt/PKB and Akt/PKB are regulated independently (Fig. 1d).

This intriguing observation prompted us to investigate the possible mechanism for this cross-talk between the Stat3 and PI(3)K-Akt/PKB pathways. The class IA PI(3)Ks are heterodimeric enzymes composed

[1]Mammary Apoptosis and Development Group, Department of Pathology, Tennis Court Road, University of Cambridge, Cambridge CB2 1QP, UK. [2]Cell Signalling Laboratory, Ludwig Institute for Cancer Research, London W1W 7BS, UK. [3]Roslin Institute, Roslin, Midlothian, EH25 9PS, UK. [4]Third Department of Internal Medicine, Faculty of Medicine, University of Tokyo, Tokyo 113, Japan. [5]Department of Biochemistry and Molecular Biology, University College London, Gower Street, London WC1E 6BT, UK.
[6]Correspondence should be addressed to C.J.W. (e-mail: cjw53@mole.bio.cam.ac.uk)

Published online: 27 March 2005; DOI: 10.1038/ncb1242

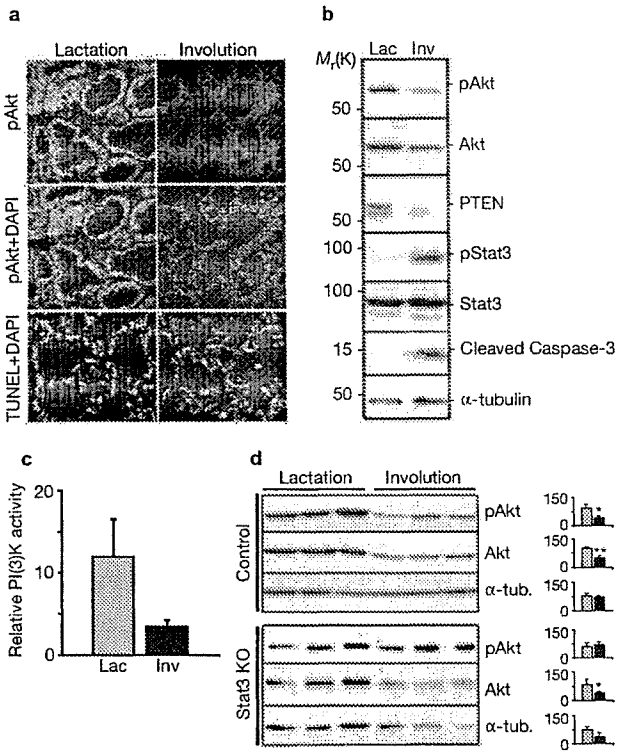

Figure 1 Activity of PI(3)K-Akt and Stat3 pathways during the apoptotic switch in mammary glands. (**a–c**) Mammary glands harvested at 10 day lactation (Lac) and 2 day involution (Inv) were analysed for (**a**) phospho-Ser473-Akt/PKB (pAkt; green) and TUNEL staining (green) by immunoflourescence of paraffin sections. Blue or red indicate nuclei. (**b**) Akt/PKB and pAkt/PKB, PTEN, Stat3 and phospho-Stat3 (Tyr701), and cleaved caspase-3 by immunoblotting and (**c**) pan-p85 antibody-associated PI(3)K activity. (**d**) Akt/PKB and pAkt/PKB as determined by immunoblot in glands from control or Stat3-deficient (Stat3 KO) glands. Each lane denotes one individual mouse. Graphs in **c** and **d** show mean ± s.d. Grey bars represent lactation, black bars represent involution. Asterisks denote statistical significance (*$P<0.05$; **$P<0.01$) in a two-tailed Student's *t*-test comparing 10-day lactation with 2-day involution. In **b** and **d**, α-tubulin was used as loading control.

of a regulatory subunit (p85α, p85β, p55α, p55γ or p50α)[10–15] and a p110 catalytic subunit (p110α, p110β or p110δ)[16,17]. Whereas p85β and p55γ are encoded by distinct genes, p85α, p55α and p50α are believed to be alternative splice forms of a single gene, *pik3r1* (refs 14, 15). Structurally, p85α, p55α and p50α share a common carboxy-terminal domain (Fig. 2a). In contrast, their amino termini are unique sequences of 340 amino acids (aa) (p85α), 34 aa (p55α) and 6 aa (p50α), respectively. It has been shown that changes in the regulatory subunit expression level can result in substantial changes in PI(3)K signalling[15,18–20]. We therefore speculated that alteration in the subunit composition of PI(3)K may be responsible for the reduced PI(3)K activity and hence the drop in pAkt/PKB during the apoptotic switch.

To investigate this hypothesis, we examined the expression of the PI(3)K regulatory subunits p85α, p85β, p55α, p55γ and p50α throughout mammary gland development, by western blot analysis using both a pan-p85 antibody and subunit-specific antibodies (Fig. 2b). The protein level of p55α was upregulated eightfold at the onset of involution, coinciding with epithelial cell apoptosis and activation of Stat3. The expression of the p50α subunit also increased during involution. In contrast, the full-length subunit p85α was substantially downregulated at the onset of involution, in a similar pattern to p85β. The expression of p55γ was constant throughout the developmental time course.

To investigate whether this marked and reciprocal expression of the three *pik3r1* splice forms p85α, p55α and p50α was occurring at the transcriptional level, we measured the levels of the individual transcripts using real-time PCR (Fig. 2c). Expression levels of p55α and p50α were upregulated approximately threefold and fivefold, respectively, by 12 h of involution. In contrast, the transcription of p85α was downregulated twofold within 24 h. This indicates that the downregulation of the p85α protein is due to transcriptional regulation and not proteolytic degradation.

Given the marked regulation of the regulatory subunits, it was important to determine whether any of the catalytic subunits were differentially expressed at the apoptotic switch. However, in contrast to the regulatory subunits, the expression of the three class IA catalytic subunits was unchanged at this time (Fig. 2d).

Thus, there is a distinct switch in the expression profile of the regulatory subunits with a marked transcriptional upregulation of p55α and p50α and downregulation of p85α, whereas the expression of p55γ and the three catalytic subunits is constant during the apoptotic switch. We have found that p55α interacts directly with p110α, p110β and p110δ (data not shown). This suggests that inducing the expression of the p55α and p50α subunits may be the means by which PI(3)K activity is regulated.

The striking correlation between the expression of the p55α and p50α subunits and the activation of Stat3 prompted us to investigate whether there is a direct connection between Stat3 activity and the induction of these two regulatory subunits. Therefore, we examined the expression of p85α, p55α and p50α in Stat3-deficient mammary glands from involuting mice (Fig. 3a). The protein levels of p55α and p50α were both significantly reduced in Stat3-deficient glands compared with controls (p55α, twofold; p50α, fourfold). In contrast, there was no significant change in the protein levels of p85α. Thus, Stat3 selectively upregulates the expression of p55α and p50α subunits in involution.

This was confirmed in tissue from LIF-deficient animals (Fig. 3b). The levels of p55α and p50α were significantly reduced in the LIF knockout mice compared with control, whereas no significant change was observed in the levels of p85α. Because the pan-p85 antibody used in these studies detects both p55α and p55γ, the levels of these subunits were determined individually. The expression of p55γ was unaltered whereas there was a significant reduction of p55α levels in LIF knockout mice. Taken together, this indicates the existence of a novel signalling pathway from LIF via Stat3 to p55α/p50α.

To examine whether Stat3 regulates the expression of p55α and p50α at the transcriptional level, we examined the mRNA level of the three *pik3r1*-encoded subunits by real-time PCR in lactating and involuting mice from Stat3-deficient and wild-type glands (Fig. 3c). *p55α* and *p50α* mRNAs were substantially upregulated in involution compared with lactation in control mice. In contrast, both *p55α* mRNA and *p50α* mRNA failed to be significantly upregulated in Stat3-deficient glands. Importantly, the levels of *p85α* mRNA were not significantly changed in the absence of Stat3.

We have previously shown that LIF-mediated activation of Stat3 induces apoptosis in a conditionally immortal mammary epithelial cell line (KIM-2)[7]. To investigate whether LIF/Stat3 could induce expression of the regulatory subunits in this cell line, we treated the cells with LIF and examined

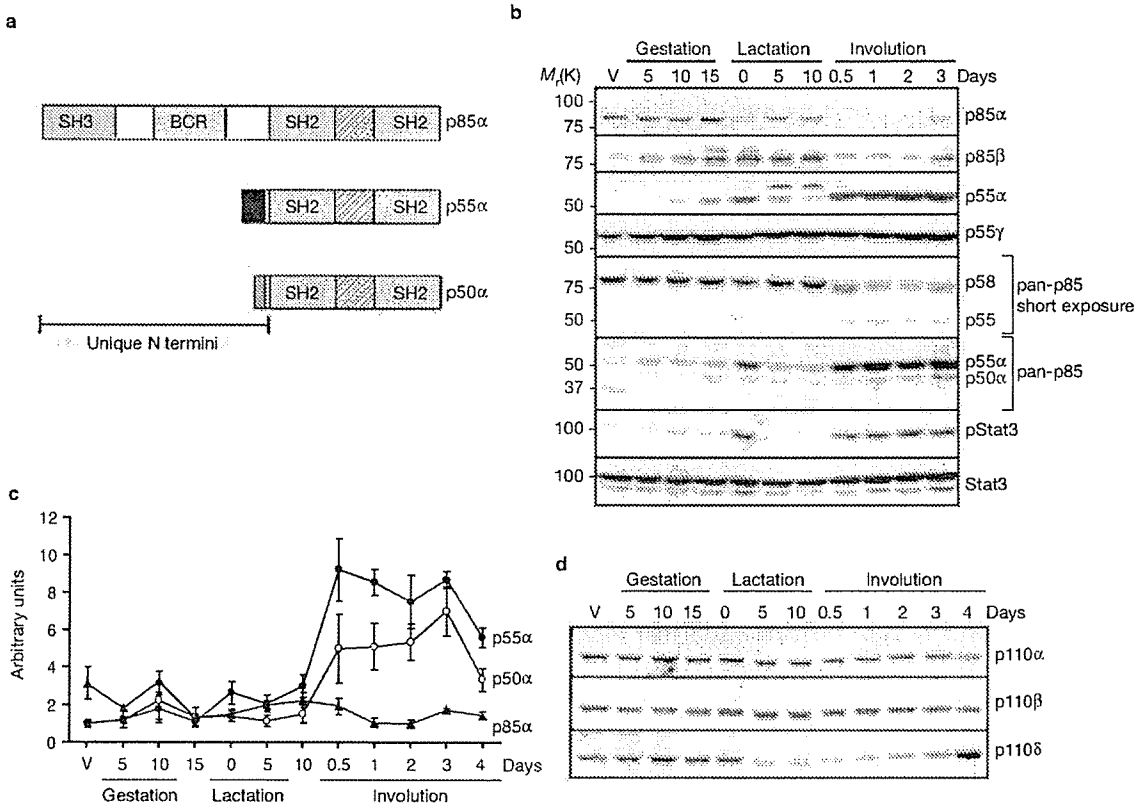

Figure 2 Differential expression of PI(3)K regulatory and catalytic subunits across the apoptotic switch. (**a**) Schematic drawing of the *pik3r1* splice forms. (**b**, **d**) Expression profiles across mammary gland development was determined by immunoblot using regulatory subunit specific antibodies (p85α, p85β, p55α, or p55γ), pan-p85 antibody (short and longer exposures) and antibodies against Stat3 and phospho-Stat3 (**b**) or catalytic subunit-specific antibodies (p110α, p110β or p110δ) (**d**). (**c**) Normalized gene expression of p85α, p55α and p50α across mammary gland development was determined by real-time PCR. Graph shows mean±s.d. In **b** and **c** the results are representative of at least three mice per time point. V, virgin mammary gland tissue.

the expression of all three subunits by immunoblotting (Fig. 3d). A twofold upregulation of p55α and an eightfold upregulation of p50α were observed after 4 h treatment with LIF, whereas no significant change in the level of p85α was detected. This was associated with cleavage of caspase-3 after 24 h. Thus, the upregulation of p55α/p50α by LIF/Stat3 is specific to epithelial cells and coincides with induction of apoptosis.

To investigate whether p55α and p50α are direct transcriptional targets of Stat3, we used the mammary epithelial cell line KIM-2 expressing an inducible Stat3–gyrase fusion protein, which allows ligand-independent dimerization and activation of Stat3 in the presence of coumermycin[21] and is associated with the induction of mammary epithelial cell apoptosis (M. B. Boland, R.W.E.C., E. A. Kritikou, J. M. Lee, T. Freeman, P.G.T. and C.J.W., unpublished observations). Induced dimerization of the Stat3-gyrase fusion protein for only 4 h resulted in a significant increase in mRNA levels of *c-fos*, a known target of Stat3 (ref. 22), *p55α* and *p50α*, whereas levels of *p85α* mRNA were unchanged (Fig. 4a). This new identification of components of the PI(3)K pathway as downstream targets of the Jak/Stat pathway is tantalizing because it couples survival and death signalling directly. The specificity of this link is emphasized further by the finding that neither *p55α* nor *p50α* mRNA expression are induced by ligand-independent activation of the related Stat5 transcription factor (data not shown). Given this rapid induction of expression, we suggest that p55α and p50α but not p85α are direct transcriptional targets of Stat3 in epithelial cells.

The LIF/Stat3 pathway is essential for self-renewal of mouse embryonic stem (ES) cells[23]. LIF mediates its effects through activation of Stat3, extracellular-signal-related kinase (ERK) and PI(3)K[24]. The mechanism of PI(3)K-mediated survival signalling is not clear. However, disruption of the *pik3r1* gene in ES cells results in undetectable levels of all three *pik3r1*-encoded transcripts and increased levels of apoptosis[25]. To investigate whether Stat3 directly induces p55α/p50α expression in ES cells, we examined the mRNA levels of the three *pik3r1* gene products in ES cells expressing a chimeric receptor that consisted of the extracellular domain of granulocyte colony-stimulating factor (G-CSF) and the intracellular domain of gp130 with a mutation of the Tyr 118 to a phenylalanine (Fig. 4b). Treatment with G-CSF, which leads to specific hyper-activation of Stat3 (ref. 23), induced transcriptional upregulation of the Stat3-target suppressor of cytokine signalling 3 (Socs3), but not p85α, p55α nor p50α. This suggests that the Stat3-p55α/p50α pathway is selective to cell types in which Stat3 induces cell death.

The selective induction of p55α/p50α expression in response to Stat3 suggests that these transcripts may be transcribed from alternate promoter(s), and are not splicing isoforms. This prompted us to examine the genomic sequence of the *pi3krl* locus. The genomic organization of the mouse *pik3r1* gene is shown in Fig. 5a. *p85α* mRNA is encoded by exon 1B and exons 2–18, *p50α* is encoded by exon 1C and exons 8–18. *p55α* is encoded by exon 1C and exons 8–18. Using *in silico* promoter

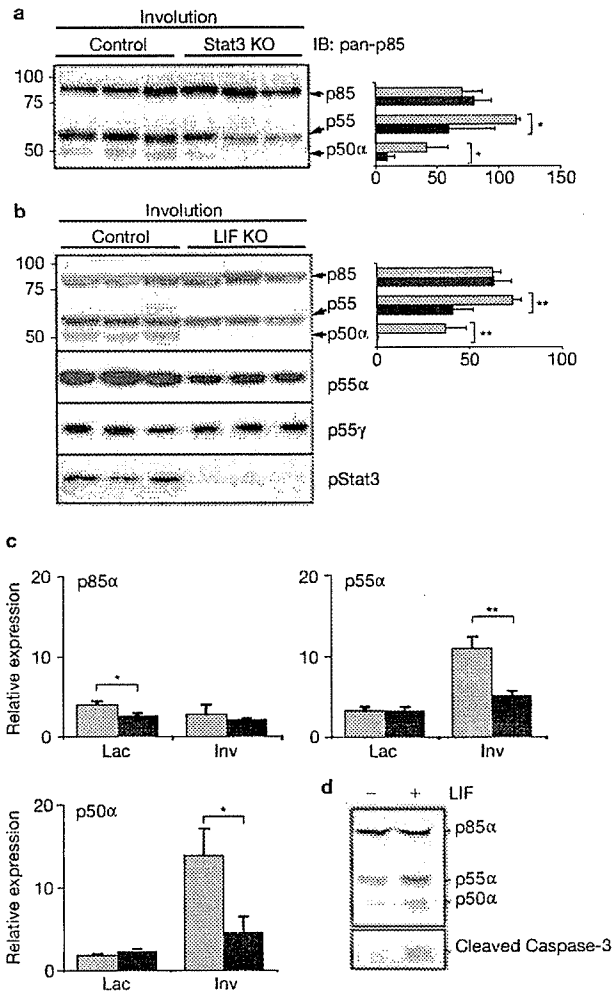

Figure 3 p55α and p50α are transcriptional targets of Stat3 *in vivo*. (**a**, **b**) p85, p55 and p50α protein expression determined by anti pan-p85 immunoblot in Stat3-knockout or anti-pan-85, anti-p55α and anti-p55γ immunoblot (**a**) and in LIF-knockout glands at 2 day involution (**b**). Each lane denotes one mouse. (**c**) Gene expression of p85α, p55α and p50α in Stat3-knockout glands from 10 day lactation and 2 day involution was determined by real-time PCR. Results are representative of at least three mice per time point. Real-time PCR results were normalized to cyclophilin mRNA. Graphs in **a**–**c** show means ± s.d. of control (grey) or test (black). Asterisks denote statistical significance (*$P<0.05$; **$P<0.01$) in a two-tailed Student's *t*-test comparing knockout to control glands. (**d**) Western blot analysis of p85, p55 and p50α expression and cleavage of caspase-3 in mammary epithelial KIM-2 cells treated with LIF for 4 h and 24 h, respectively.

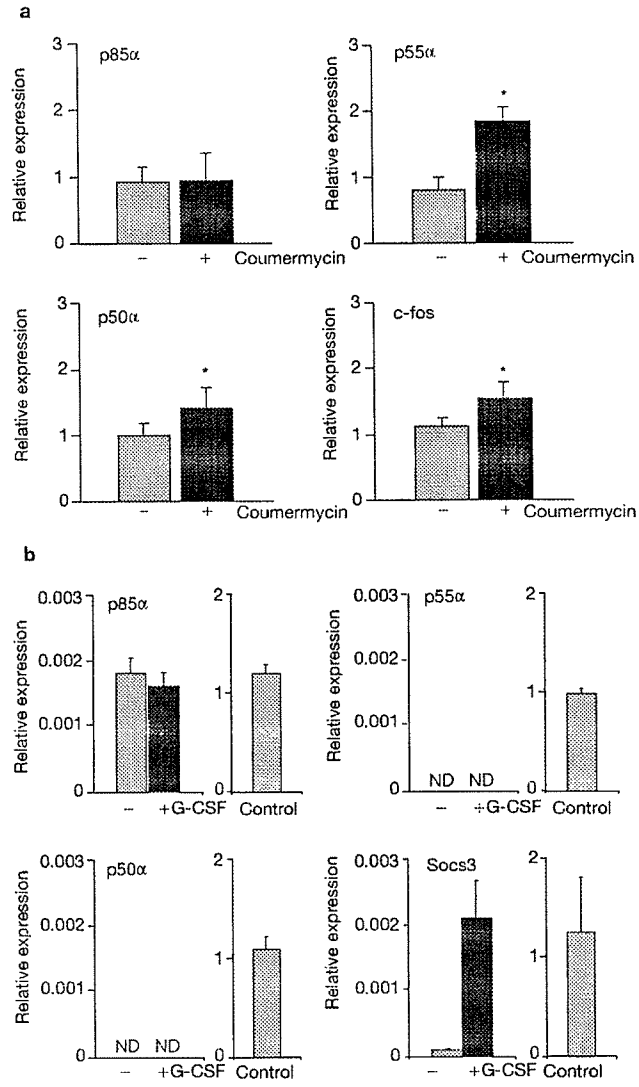

Figure 4 Stat3 regulates transcription of p55α and p50α in mammary, but not ES cells. (**a**) Transcription of p85α, p55α, p50α and c-fos in Stat3-GyrB-KIM-2 cells untreated (grey) or treated with coumermycin for 4 h (black) as determined by real-time PCR. (**b**) Gene expression of p85α, p55α, p50α and Socs3 in G-CSF-gp130-expressing ES cells untreated (grey) or treated with G-CSF for 1 h (black) as determined by real-time PCR. A pool of lactation and involution mammary gland cDNA was used as positive control. ND, not detectable. Real-time PCR results were normalized to cyclophilin mRNA. Graphs show means ± s.d. of control (grey) or test (black). Asterisks denote statistical significance (*$P<0.05$) in a two-tailed Student's *t*-test comparing treated versus untreated cells.

prediction tools, and information on 5′ cap sites, we have identified putative promoter regions 5′ flanking to exon 1A (p85α), 1B (p50α) and 1C (p55α), respectively. The potential p85α promoter contains a CpG island and several GC-boxes, and p50α a CpG island, whereas the potential p55α promoter contains a putative initiator consensus at the transcription start site. Potential Stat-binding motifs are present within the putative promoter regions of both p55α and p50α. To examine whether these Stat sites bind Stat3 *in vivo*, we performed chromatin immunoprecipitation (ChIP) assay in glands from lactating and involuting mice using promoter-specific primers and real-time PCR (Fig. 5b). The ChIP assay shows that Stat3 binds to the Stat consensus sequence in both the p50α and the p55α promoters *in vivo* in the involuting gland. Interestingly, Stat3 is associated with the promoter region of p50α in both lactation and involution. Because levels of unphosphorylated Stat3 are high in lactation (Fig. 1b), this indicates that the promoter region of p50α can be preloaded with inactive Stat3. Dynamic shuttling of unphosphorylated Stats 1, 2 and 3 is well documented and we have evidence of the presence of unphosphorylated Stat3 in nuclear extracts from lactating mammary gland (data not shown). We suggest that activation of Stat3 in involution by LIF results in the displacement of inactive Stat3 and transcriptional activation of p50α. In contrast, the p55α promoter only binds Stat3 in involution, providing